ISINN-29

VORONEZH STATE UNIVERSITY

P-even T-odd asymmetries in nuclear fission reactions by polarized neutrons with the emission of different light particles

Lyubashevsky D.E., Kadmensky S.G.

Dubna - 2023

Section 1

Description of P-even T-odd asymmetries in differential cross sections for fission reactions of unoriented target nuclei by cold polarized neutrons with the emission of prescission and evaporative light particles through triple and quintuple correlators in the indicated cross sections.

F. Goennenwein, M. Mutterer, J. von Kalben, et al // Phys. Lett. B. 2007. V.652. P.13.

A. Gagarski , I. Guseva ,G. Petrov, et al // Phys. Rev. 2016. V. 93. P. 054619.

Г.В. Данилян, Й. Кленке, Ю.Н. Копач и др. // ЯФ. 2014. Т. 77. С. 715.

Jessinger P., Danilyan G. V., Gagarski A.M. et al. // Physics of Atomic Nuclei 1999. V. 62. P. 1608-1610.

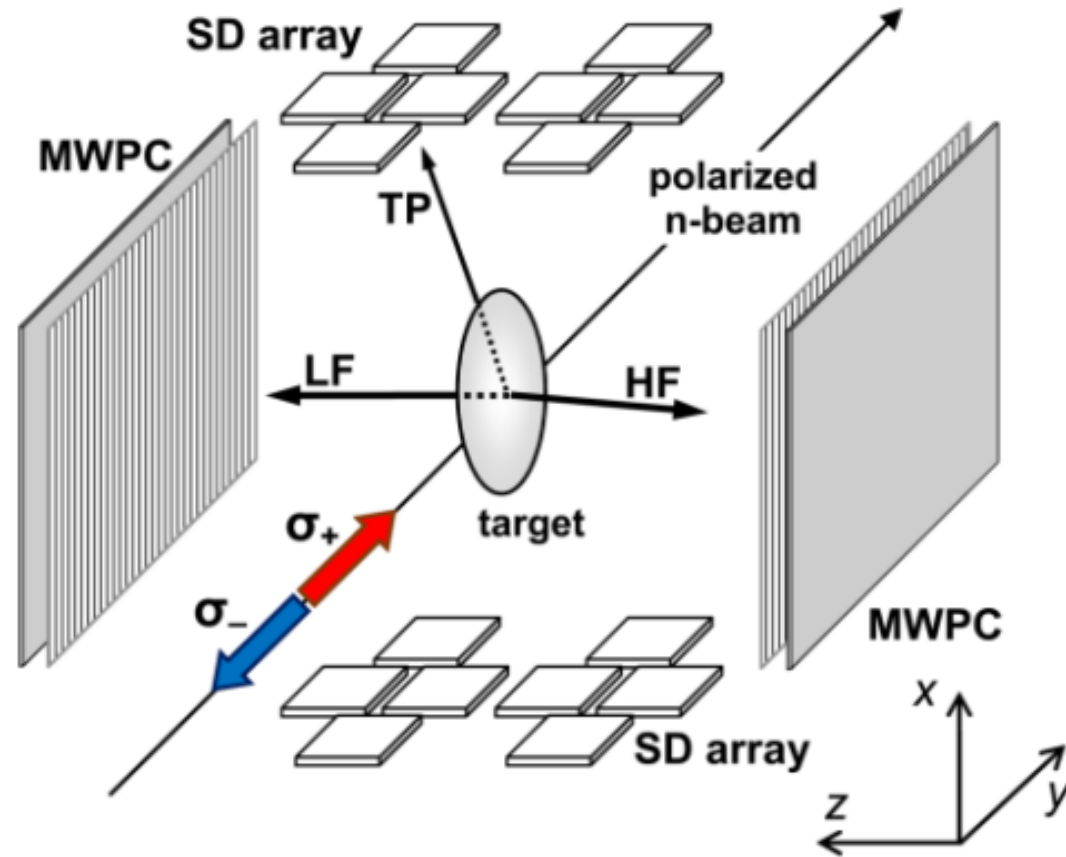.В. Вальский, А.М. Гагарский, И.С. Гусева и др. // Изв.РАН, Сер.физ. 2010, Т.74, 803.

Fig. 1. Scheme of the experimental setup.

A. Gagarski , I. Guseva ,G. Petrov, et al // Phys. Rev. 2016. V. 93. P. 054619.

$$d\sigma_{nf,p}(\theta)\big/d\Omega = d\sigma_{nf,p}^{\{0\}}(\theta)\big/d\Omega + d\sigma_{nf,p}^{\{1\}}(\theta)\big/d\Omega, \quad \text{(1)}$$

$$\left(\mathbf{k}_{LF}, \mathbf{k}_p\right)^n = \cos^n(\theta) \quad \text{(2)}$$

$$d\sigma_{nf,p}^{\{0\}}(\theta)\big/d\Omega = \sigma_{nf,p}^{\{0\}}P_p^{\{0\}}(\theta), \quad \text{(3)}$$

where $\sigma_{nf,p}^{\{0\}}$ is the total cross section of the reaction under study, and $P_p^{\{0\}}(\theta)$ is the angular distribution of emitted light particles p.

$$\int\limits_{0}^{2\pi}\int\limits_{0}^{\pi} P_p^{\{0\}}(\theta)\sin\theta d\theta d\varphi = 1.$$

(4)

$$P_\alpha^{\{0\}}(\theta) = K_\alpha \exp\left\{-\frac{1}{2}\left((\theta-\theta_0)/a\right)^2\right\}.$$

(5)

$$P_{n',\gamma}^{\{0\}}(\theta) = K_{n',\gamma}\left(1 + A_{n',\gamma}\cos^2\quad,\right.$$

(6)

C. Guet, C. Signarbrieux, P. Perrin, H. N[IFenecker, et al. // Nucl.Phys. A314 (1979) 1 – 26. F. Fossati, C. Petronio and T. Pinelli. // Nucl. Phys., A 208 (1973) 196-206.

B. M. Струтинский // ЖЭТФ. 1959. Т. 37. С. 861.

T. Ericson, and V. Strutinsky // Nucl. Phys. 8, 284 (1958).

Table 1

Target nucleus	θ_0	a	K_α	$K_{n'}$	K_γ	$A_{n'}$	A_γ
^{233}U	82	9.35	0.043	0.300	0.295	0.1	0.146
^{235}U	82	10.2	0.039	0.300	0.295	0.1	0.146
^{239}Pu	83	11	0.036				
^{241}Pu	83	10.2	0.039				

$$d\sigma^{\{1\}}_{nf,p}(\theta)\big/d\Omega = \left(d\sigma^{\{1\}}_{nf,p}(\theta)\big/d\Omega\right)_3 + \left(d\sigma^{\{1\}}_{nf,p}(\theta)\big/d\Omega\right)_5, \qquad (7)$$

$$\left(d\sigma^{\{1\}}_{nf,p}(\theta)\big/d\Omega\right)_3 = B_3(\theta)\left(\boldsymbol{\sigma}_n\left[\mathbf{k}_{LF},\mathbf{k}_p\right]\right), \qquad (8)$$

$$\left(d\sigma^{\{1\}}_{nf,p}(\theta)\big/d\Omega\right)_5 = B_5(\theta)\left(\boldsymbol{\sigma}_n\left[\mathbf{k}_{LF},\mathbf{k}_p\right]\right)\left(\mathbf{k}_{LF},\mathbf{k}_p\right). \qquad (9)$$

С.Г. Кадменский, Д.Е. Любашевский, П.В. Кострюков / Связь экспериментальных характеристик P-чётных T-нечётных асимметрий в тройном делении ядер холодными поляризованными нейтронами с тройными и пятерными скалярными корреляциями // Ядерная физика .— 2019.— Т. 82, № 3. - С. 252-259.

$$\left(d\sigma_{nf,p}^{\{1\}}\left(\theta\right)\Big/ d\Omega \right)_3 = B_3\left(\theta\right)\left|\boldsymbol{\sigma}_n\right|\sin\left(\theta\right),$$

(10)

$$\left(d\sigma_{nf,p}^{\{1\}}\left(\theta\right)\Big/ d\Omega \right)_5 = B_5\left(\theta\right)\left|\boldsymbol{\sigma}_n\right|\cos\left(\theta\right)\sin\left(\theta\right),$$

(11)

$$\left(d\sigma_{nf,p}^{\{1\}}\left(\theta\right)\Big/ d\Omega \right)_{3(5)} = \left(d\sigma_{nf,p}^{\{1\}}\left(\theta\right)\Big/ d\Omega \right)_{ev(odd)} = \frac{1}{2}\left(d\sigma_{nf,p}^{\{1\}}\left(\theta\right)\Big/ d\Omega \pm d\sigma_{nf,p}^{\{1\}}\left(\pi-\theta\right)\Big/ d\Omega \right).$$

(12)

$$D_{nf,p}(\theta) = \left(N_p^+(\theta) - N_p^-(\theta) \right) \Big/ \left(N_p^+(\theta) + N_p^-(\theta) \right), \qquad (13)$$

where $N_p^\pm(\theta)$ - particle count rates p in coincidence with light fission fragments for the directions of the polarization vector of the incident neutron spin $\boldsymbol{\sigma}_n^+$ or $\boldsymbol{\sigma}_n^-$.

$$D_{nf,p}(\theta) = \left(d\sigma_{nf,p}^{\{1+\}}(\theta) \Big/ d\Omega \right) \Big/ \left(d\sigma_{nf,p}^{\{0+\}}(\theta) \Big/ d\Omega \right). \qquad (14)$$

$$d\sigma_{nf,p}^{\{1+\}}(\theta)/d\Omega = D_{nf,p}(\theta)\left(d\sigma_{nf,p}^{\{0\}}(\theta)/d\Omega\right), \tag{15}$$

$$\left(d\sigma_{nf,p}^{\{1+\}}(\theta)/d\Omega\right)_{3(5)} = \left(D_{nf,p}(\theta)d\sigma_{nf,p}^{\{0\}}(\theta)/d\Omega\right)_{ev(odd)}. \tag{16}$$

$$\left(\beta_{nf,p}(\theta)\right)_{3(5)} \equiv \left(d\sigma_{nf,p}^{\{1+\}}(\theta)/d\Omega\right)_{3(5)} \Big/ \sigma_{nf,p}^{\{0\}}, \tag{17}$$

$$\left(\beta_{nf,p}(\theta)\right)_{3} = \left(D_{nf,p}(\theta)P_{p}^{\{0\}}(\theta)\right)_{ev}, \tag{18}$$

$$\left(\beta_{nf,p}(\theta)\right)_{5} = \left(D_{nf,p}(\theta)P_{p}^{\{0\}}(\theta)\right)_{odd}. \tag{19}$$
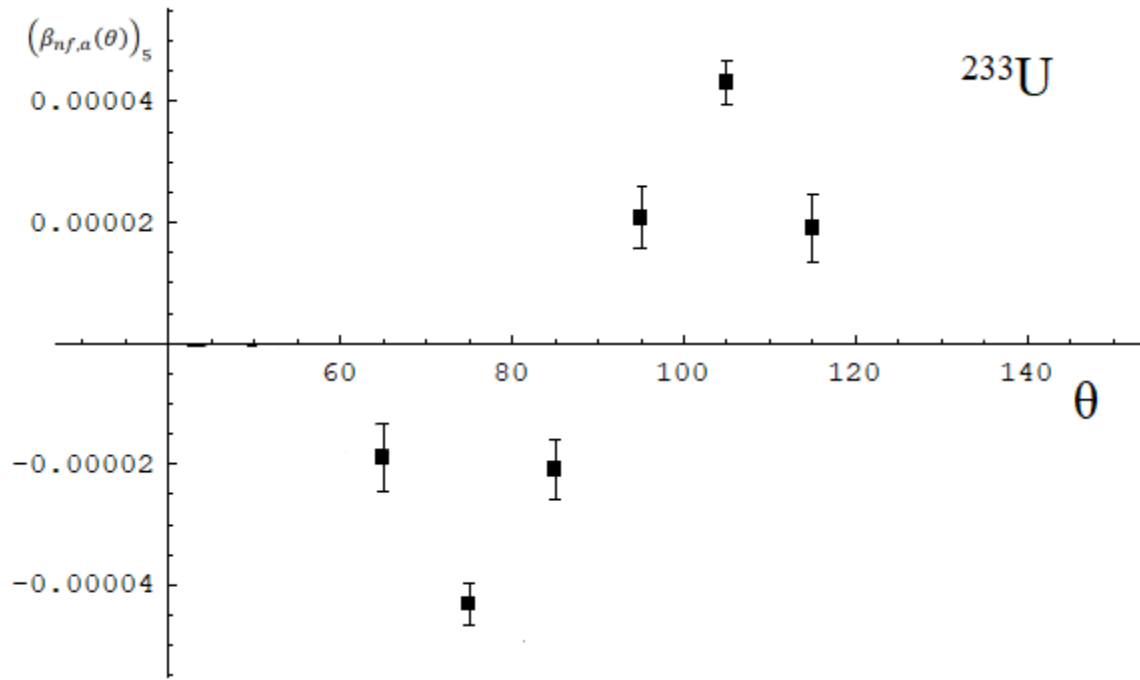
Fig. 2. Experimental (black squares) values of quantity $\left(\beta_{nf,\alpha}(\theta)\right)_5$ in the case of the ^{233}U target nucleus.
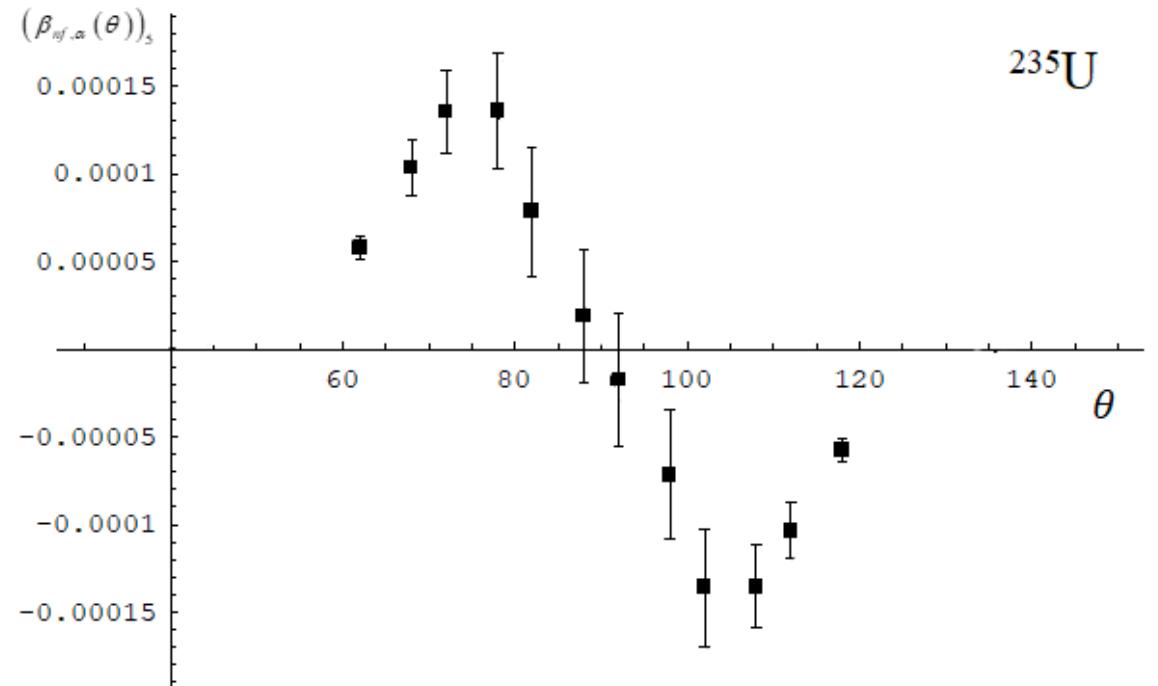
Fig. 3. Experimental (black squares) values of quantity $\left(\beta_{nf,\alpha}(\theta)\right)_5$ in the case of the ^{235}U target nucleus.
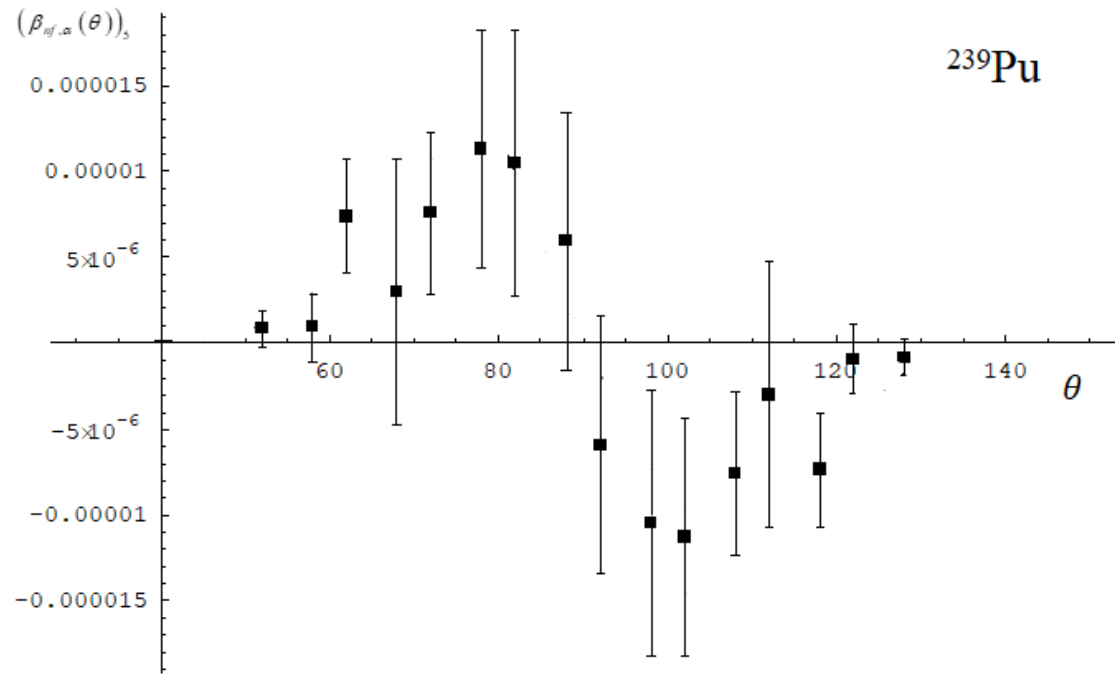
Fig. 4. Experimental (black squares) values of quantity $\left(\beta_{nf,\alpha}(\theta)\right)_s$ in the case of the ^{239}Pu target nucleus.
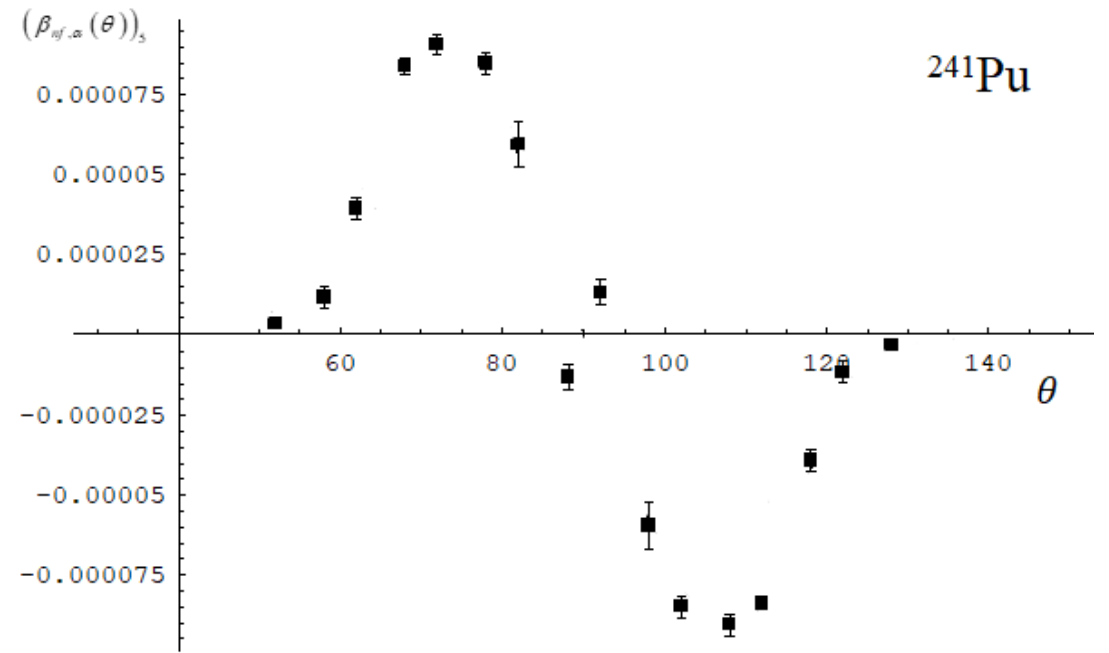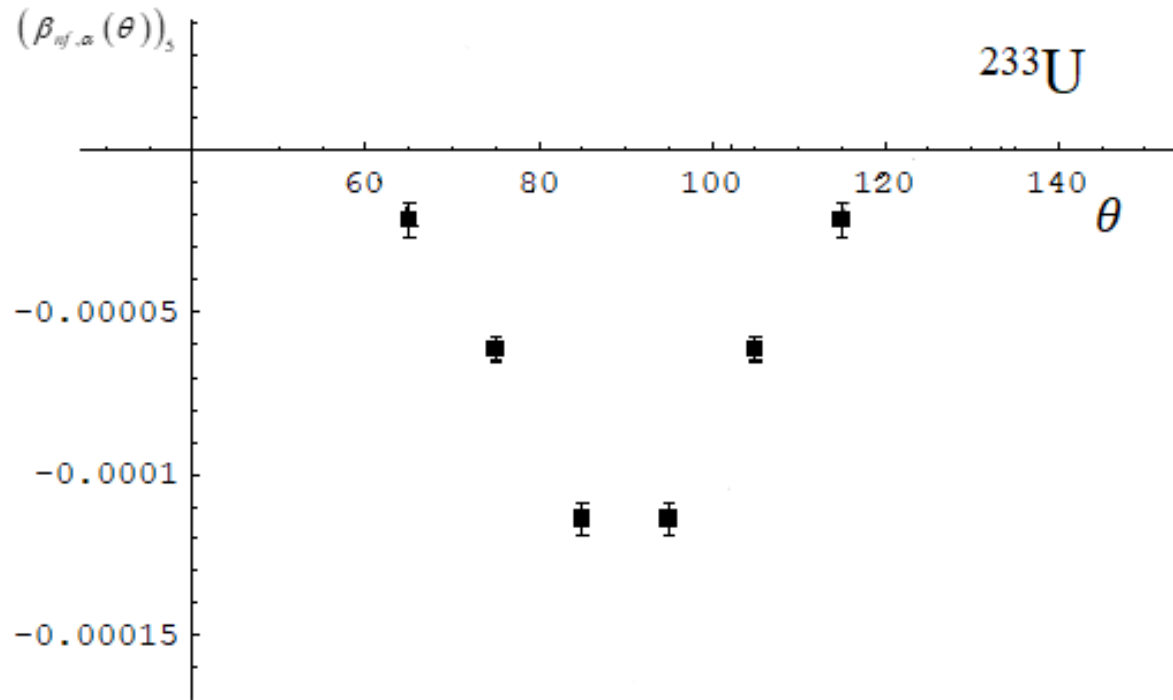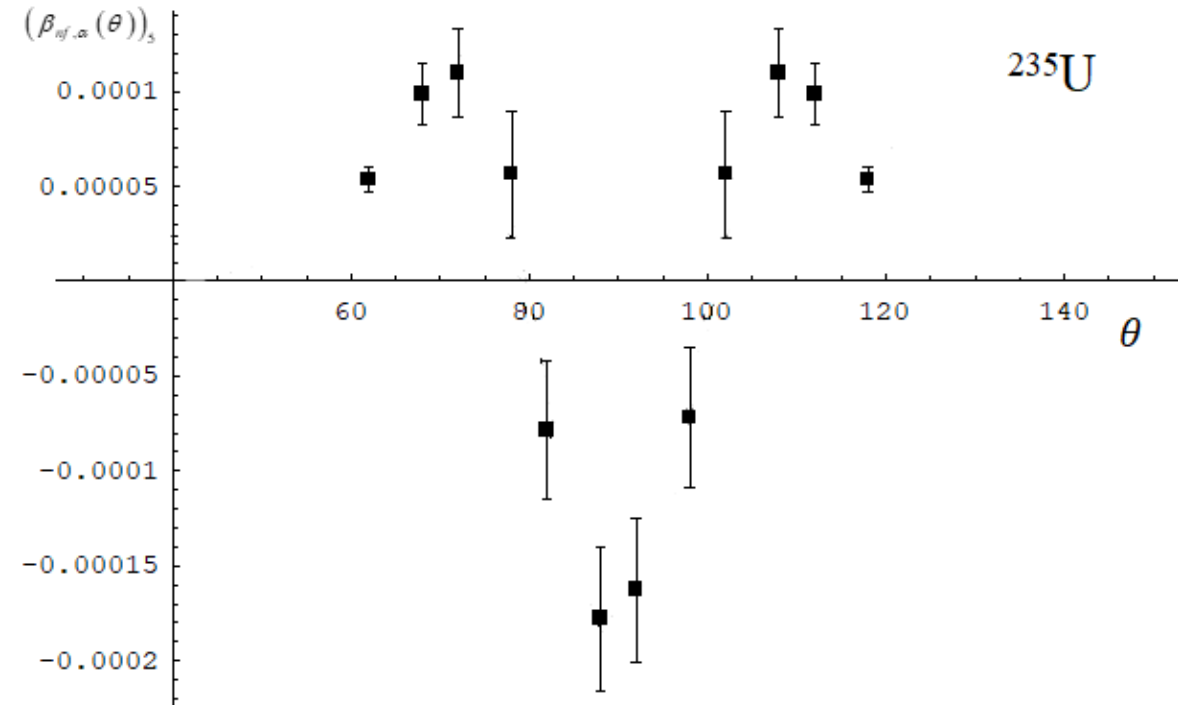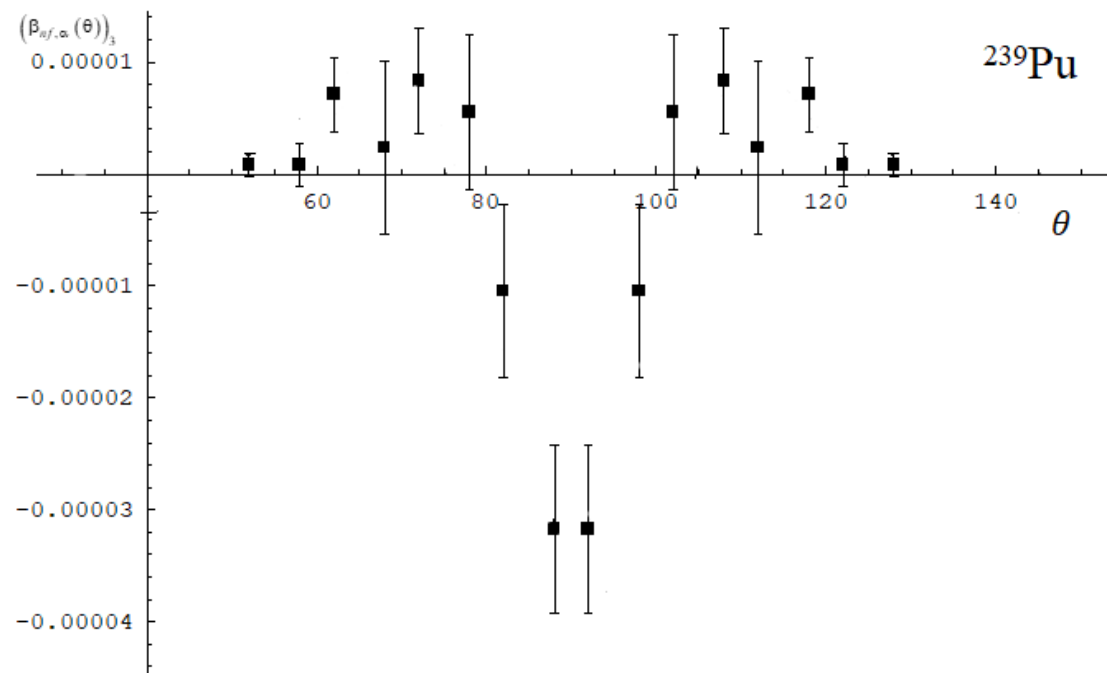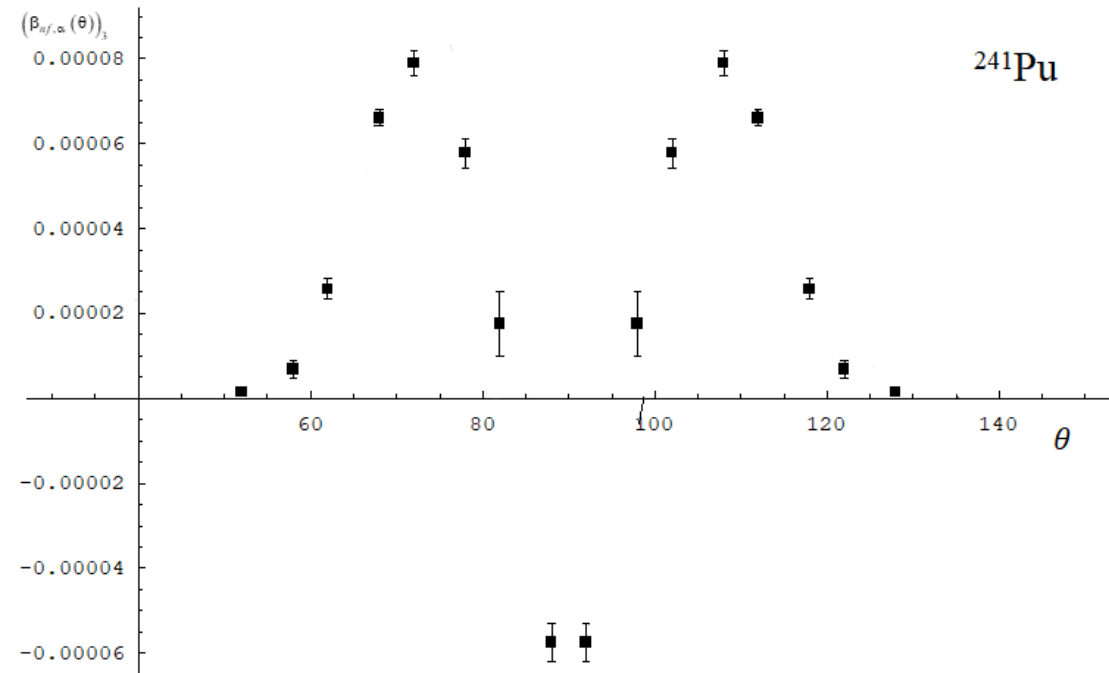

Fig. 5. Experimental (black squares) values of quantity $\left(\beta_{nf,\alpha}(\theta)\right)_s$ in the case of the ^{241}Pu target nucleus.

Fig. 6. Experimental (black squares) values of quantity $\left(\beta_{nf,\alpha}(\theta)\right)_3$ in the case of the ^{233}U target nucleus.

Fig. 7. Experimental (black squares) values of quantity $\left(\beta_{nf,\alpha}(\theta)\right)_3$ in the case of the ^{235}U target nucleus.

Fig. 8. Experimental (black squares) values of quantity $\left(\beta_{nf,\alpha}(\theta)\right)_3$ in the case of the ^{239}Pu target nucleus.

Fig. 9. Experimental (black squares) values of quantity $\left(\beta_{nf,\alpha}(\theta)\right)_3$ in the case of the ^{241}Pu target nucleus.
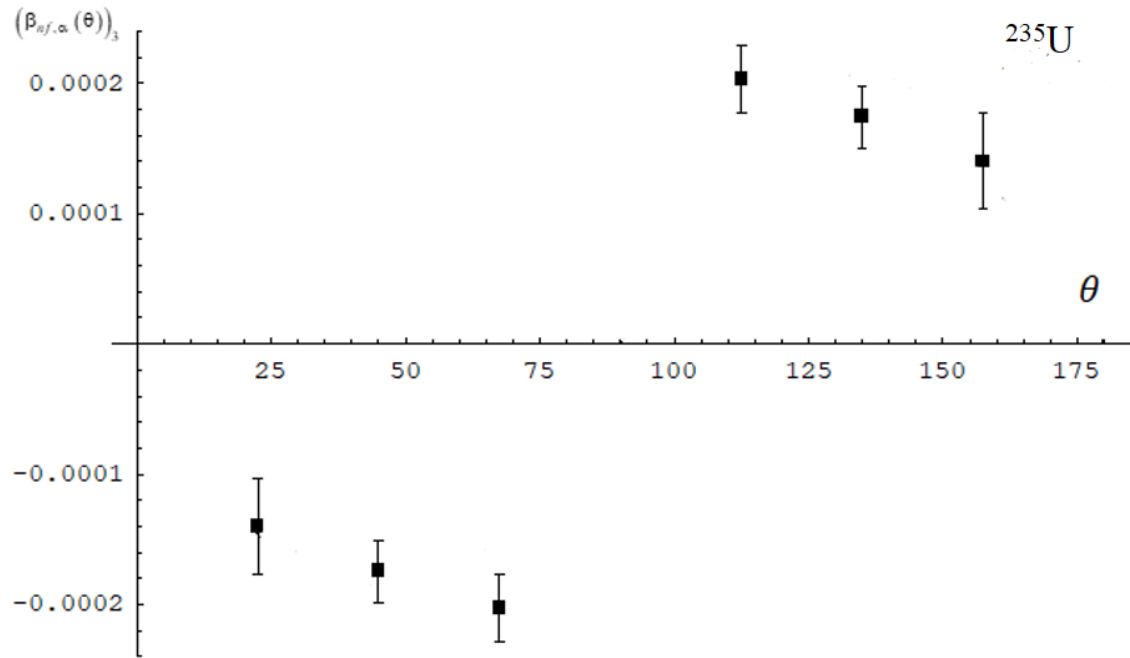
Fig. 10. Experimental (black squares) values of quantity $\left(\beta_{nf,\gamma}(\theta)\right)_5$ in the case of the ^{235}U target nucleus.
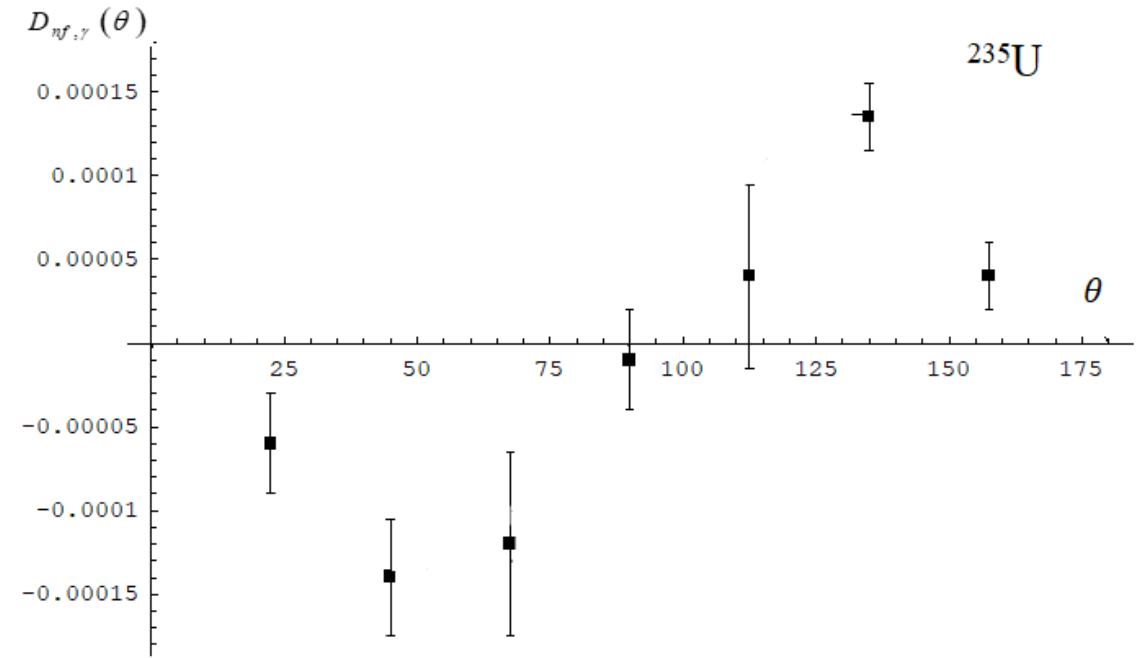

Fig. 11. Experimental (black squares) coefficients of asymmetry $D_{nf,\gamma}(\theta)$ in the case of the ^{235}U target nucleus.
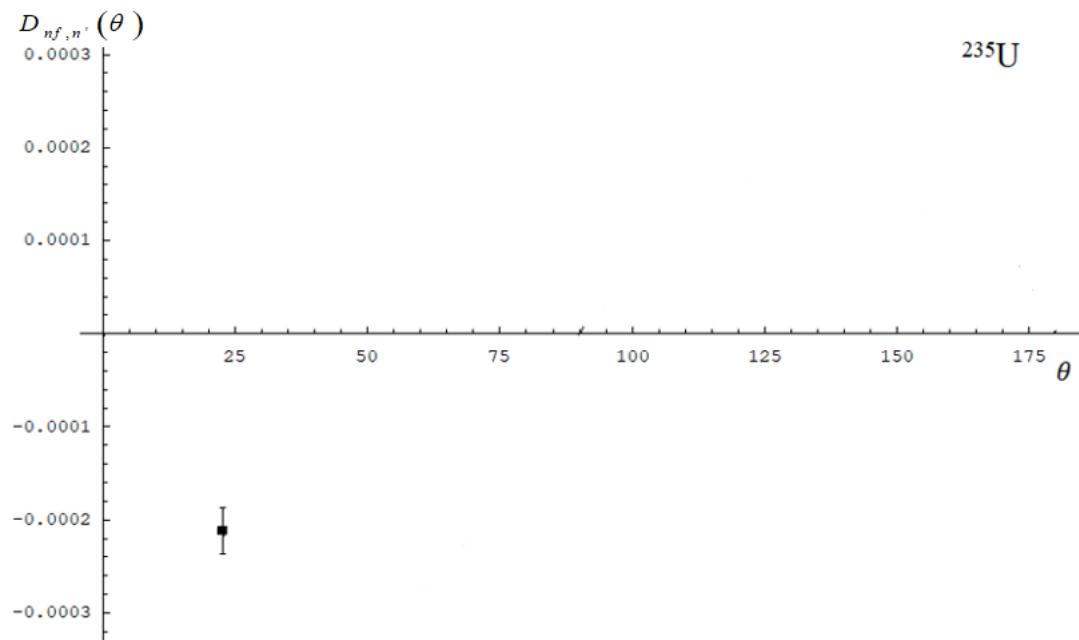
Fig. 12. Experimental (black squares) coefficients of asymmetry $D_{nf,n'}(\theta)$ in the case of the ^{235}U target nucleus.
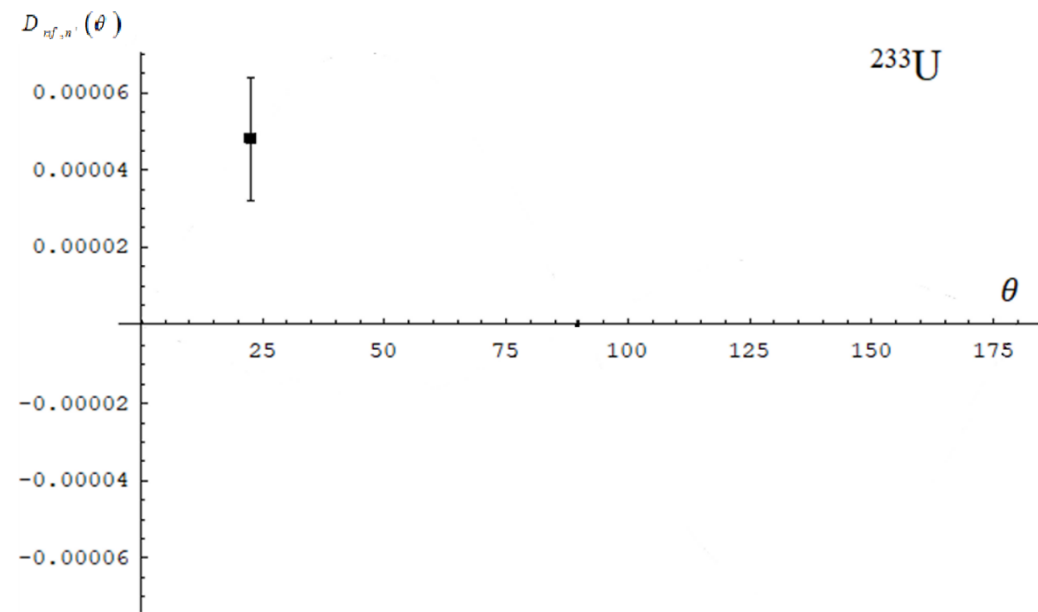

Fig. 13. Experimental (black squares) coefficients of asymmetry $D_{nf,n'}(\theta)$ in the case of the ^{233}U target nucleus.
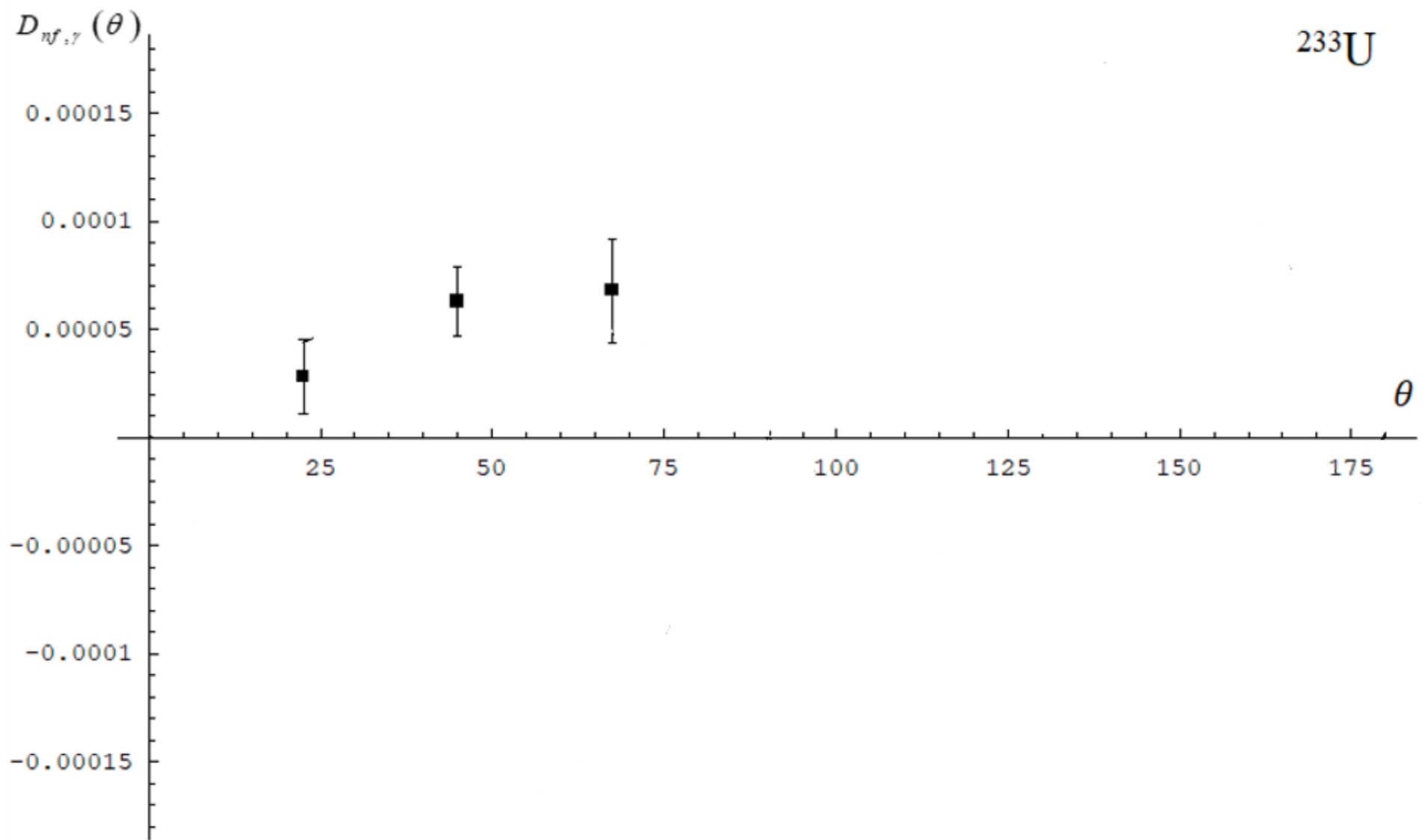
Fig. 14. Experimental coefficients of asymmetry $D_{nf,\gamma}(\theta)$ in the case of the ^{233}U target nucleus.

Section 2

Problems of describing P-even T-odd asymmetries in fission reactions of unoriented target nuclei by cold polarized neutrons with the emission of prescission and evaporative light particles using the semiclassical method of trajectory calculations.

$$D_{nf,\alpha}\left(\theta\right) = \Delta_\alpha \cdot \frac{d\left(d\sigma_{nf,\alpha}^{\{0\}}\left(\theta\right)\middle/d\Omega\right)}{d\theta} \middle/ \left(d\sigma_{nf,\alpha}^{\{0\}}\left(\theta\right)\middle/d\Omega\right) + D_{TRI},\tag{20}$$

$$D_{nf,\alpha}\left(\theta\right) = \Delta_\alpha \cdot \frac{dP_\alpha^{\{0\}}\left(\theta\right)}{d\theta} \middle/ P_\alpha^{\{0\}}\left(\theta\right) + D_{TRI}.\tag{21}$$

A. Gagarski , I. Guseva ,G. Petrov, et al // Phys. Rev. 2016. V. 93. P. 054619.

$$\Delta_\alpha = \Delta_{LF} - \Delta_\alpha^0, \qquad\qquad (22)$$

where Δ_{LF} and Δ_α are the angles of rotation under the influence of the Coriolis interaction of the wave vectors of the light fission fragment $\mathbf{k}_{LF}$ and the alpha particle $\mathbf{k}_\alpha$.

F. Goennenwein, M. Mutterer, J. von Kalben, et al // Phys. Lett. B. 2007. V.652. P.13.
A.Gagarski , I. Guseva ,G. Petrov, et al // Phys. Rev. 2016. V. 93. P. 054619.
Гусева И.С., Гусев Ю.И. // Изв. РАН. Сер. физ. 2007. Т. 71. С. 382
A. M. Gagarski, I. S. Guseva, F. Goennenwein et al. // Crystallography Reports, 2011, Vol. 56, No. 7, pp. 1238. DOI: 10.1134/S1063774511070133
Г.В. Вальский, А.М. Гагарский, И.С. Гусева и др. // Изв.РАН, Сер.физ. 2010, Т.74, 803.

Table 2

Target nucleus	$D_{TRI} \times 10^{-3}$	$\Delta_\alpha \times 10^{-3}$
^{233}U	-3.90	0.18
^{235}U	1.72	1.9
^{239}Pu	-0.23	0.17
^{241}Pu	1.30	0.41

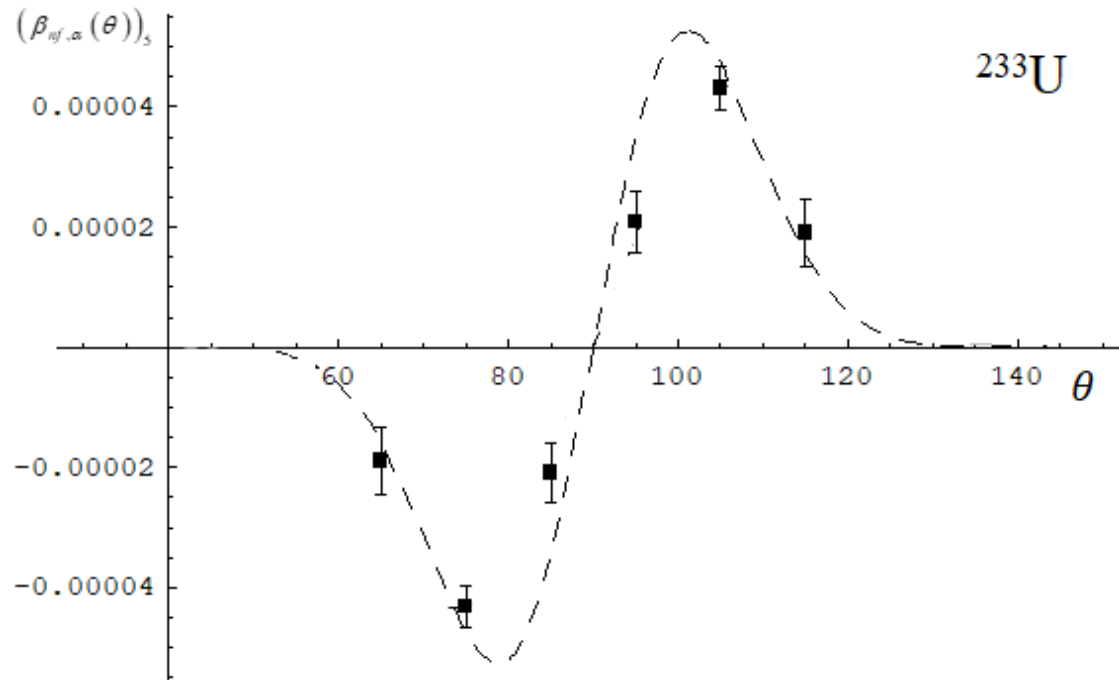Fig. 15. Experimental (black squares) and calculated (short dotted line - semiclassical approach) values of $\left(\beta_{nf,\alpha}(\theta)\right)_5$ in the case of the ^{233}U target nucleus.
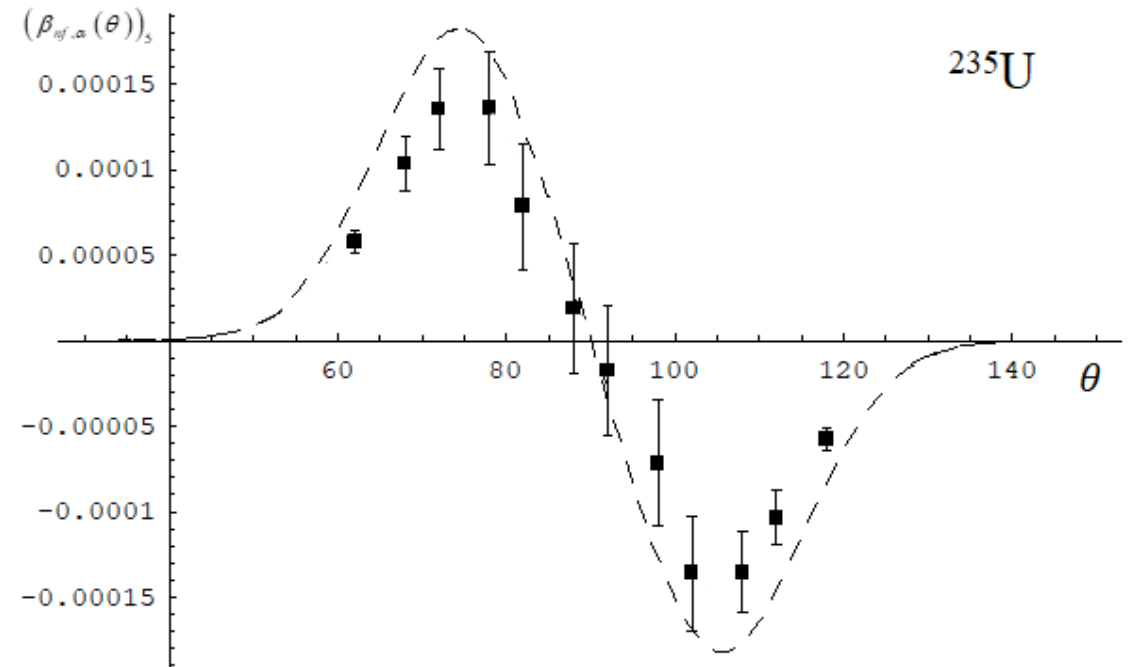
Fig. 16. Experimental (black squares) and calculated (short dashed line – semiclassical approach and long dashed line – quantum approach) values of $\left(\beta_{nf,\alpha}(\theta)\right)_5$ in the case of the ^{235}U target nucleus.
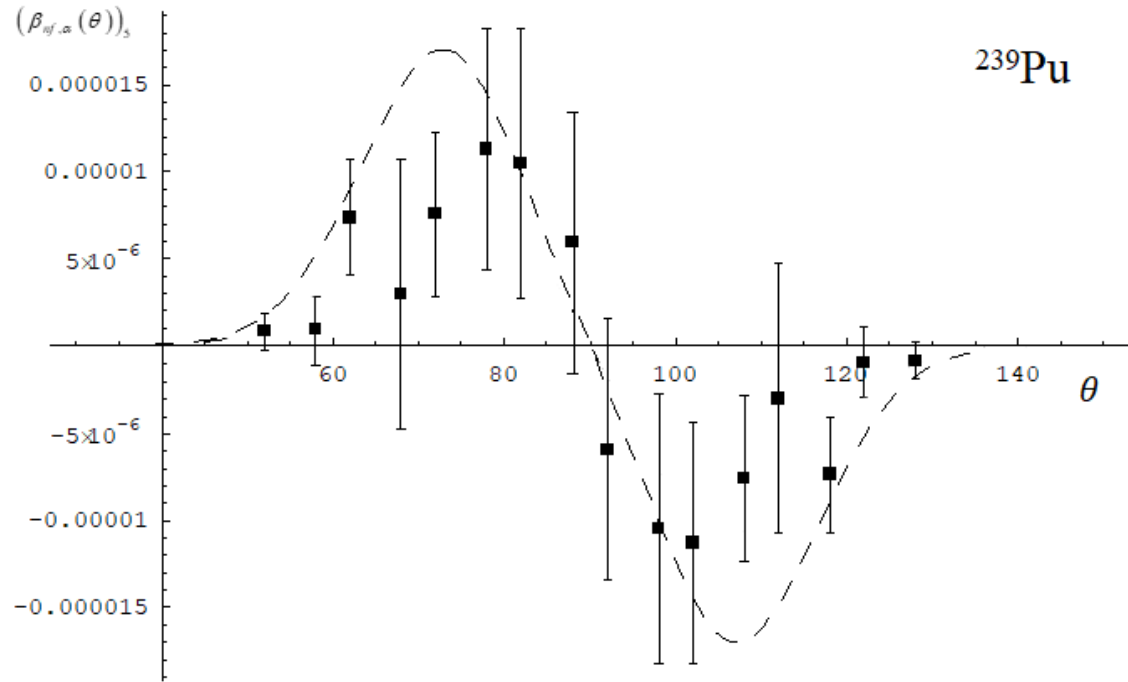
Fig. 17. Experimental (black squares) and calculated (short dotted line - semiclassical approach) values of $\left(\beta_{nf,\alpha}(\theta)\right)_5$ in the case of the target nucleus ^{239}Pu.

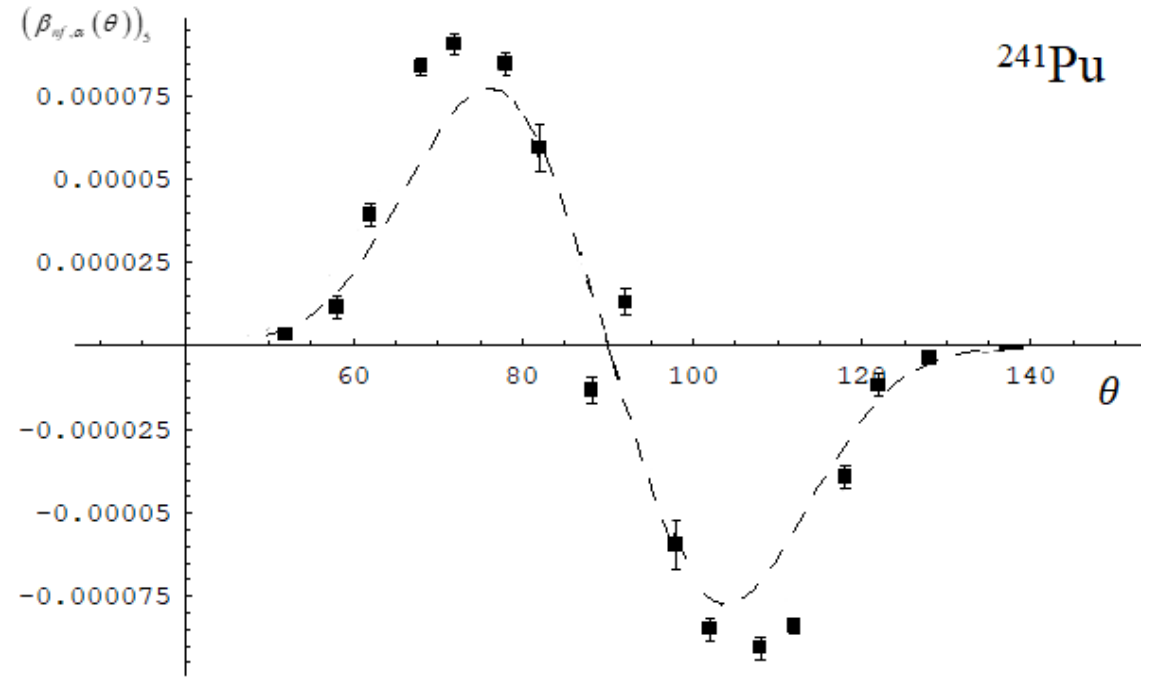Fig. 18. Experimental (black squares) and calculated (short dotted line - semiclassical approach) values of $\left(\beta_{nf,\alpha}(\theta)\right)_5$ in the case of the target nucleus ^{241}Pu.

Fig. 19. Experimental (black squares) and calculated (short dotted line - semiclassical approach) values of $\left(\beta_{nf,\alpha}(\theta)\right)_3$ in the case of the ^{233}U target nucleus.
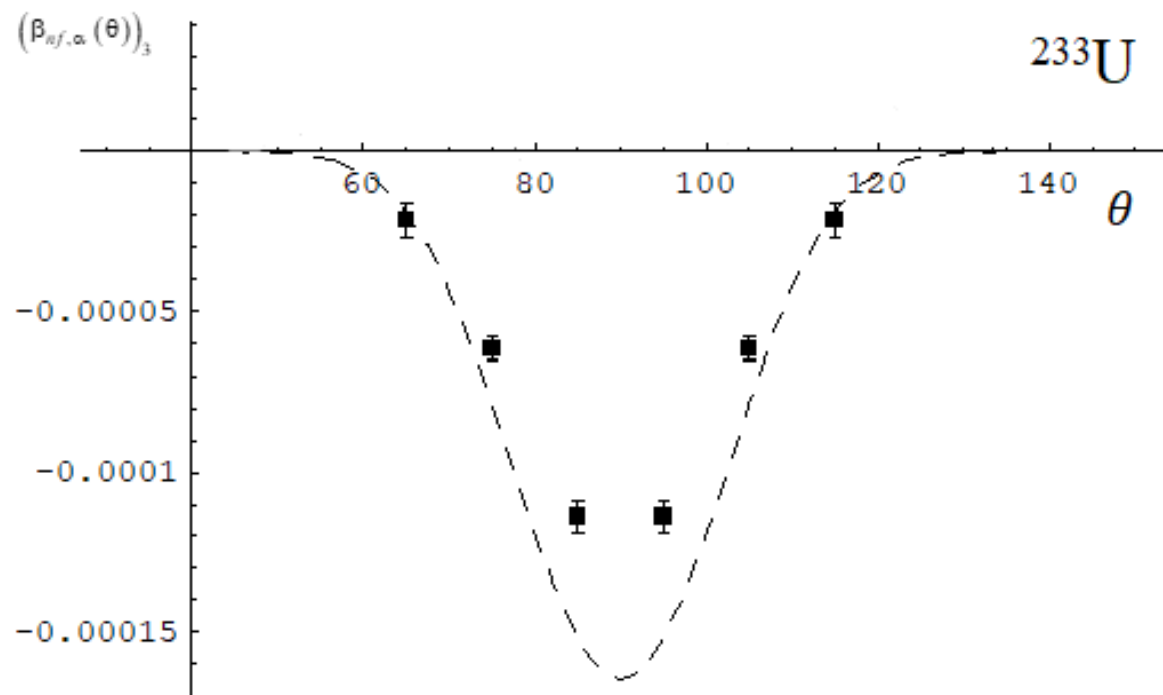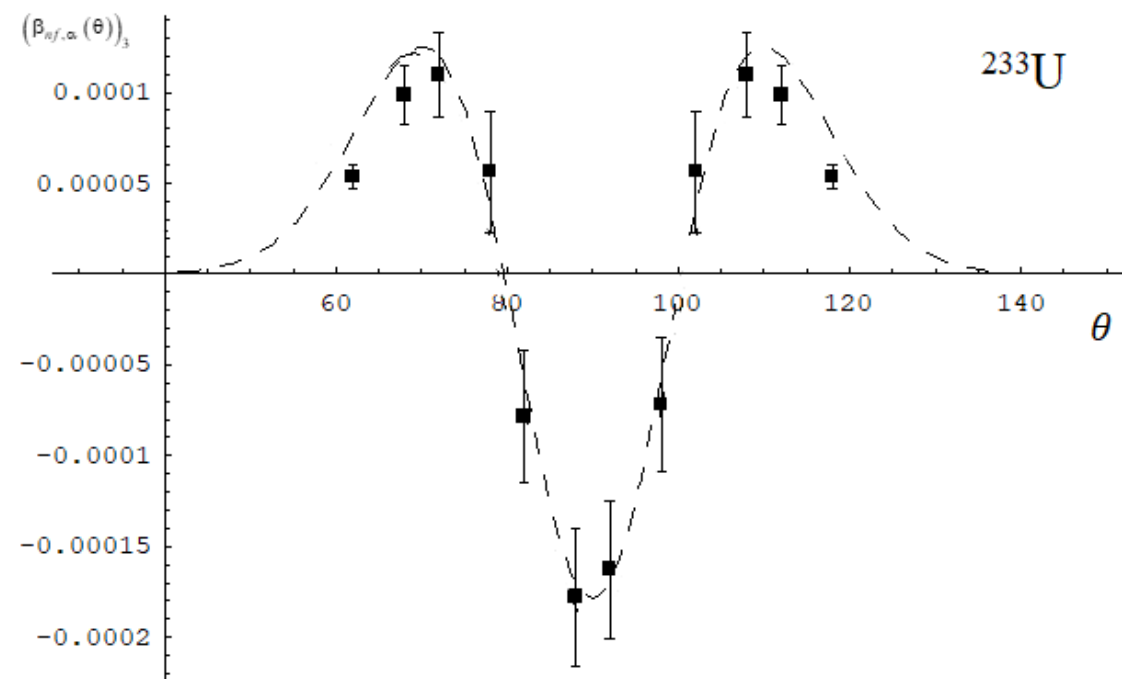
Fig. 20. Experimental (black squares) and calculated (short dotted line - semiclassical approach) $\left(\beta_{nf,\alpha}(\theta)\right)_3$ in the case of the ^{235}U target nucleus.

Fig. 21. Experimental (black squares) and calculated (short dotted line - semiclassical approach) values of $\left(\beta_{nf,\alpha}(\theta)\right)_3$ in the case of the ^{239}Pu target nucleus.

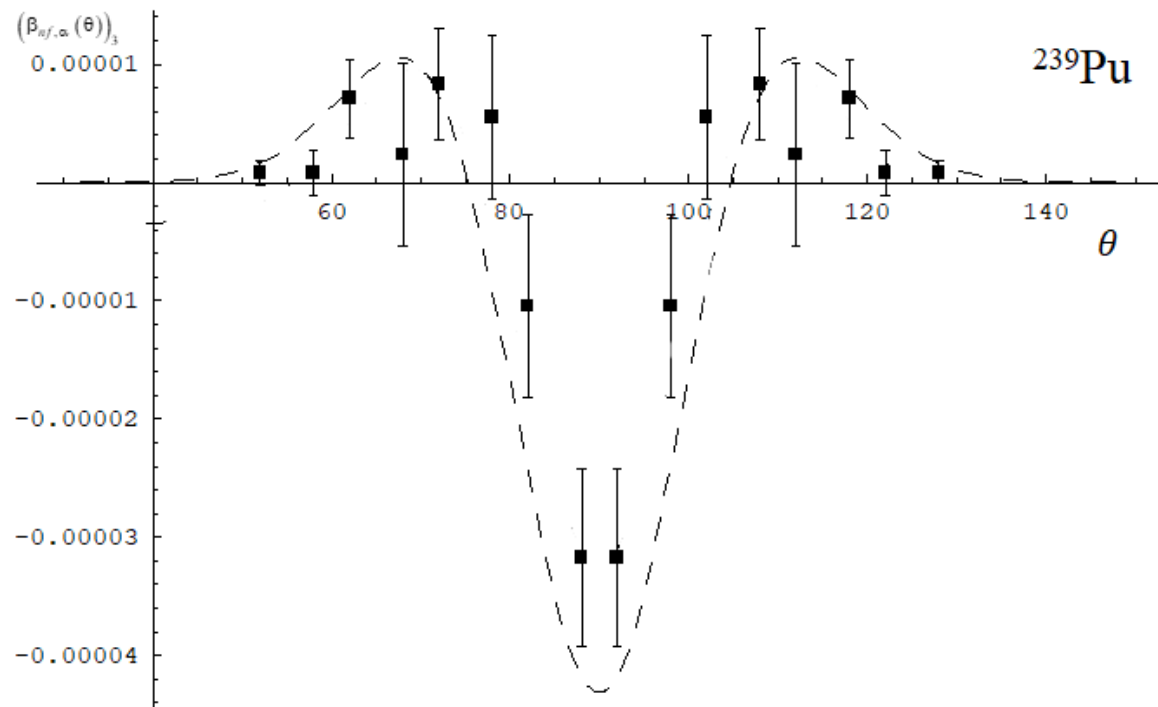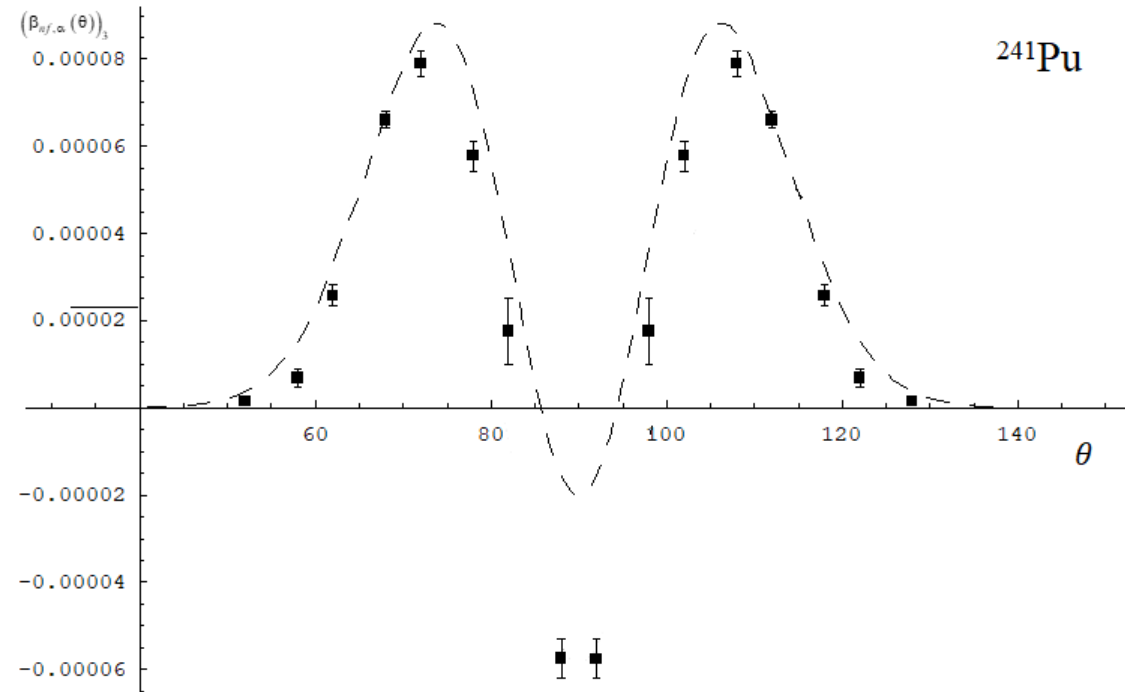Fig. 22. Experimental (black squares) and calculated (short dotted line – semiclassical approach) values of $\left(\beta_{nf,\alpha}(\theta)\right)_3$ in the case of the ^{241}Pu target nucleus.

Then the formula for describing the coefficients $D_{nf,n'}(\theta)$ and $D_{nf,\gamma}(\theta)$ in the semiclassical approach turns into the formula:

$$D_{nf,n'(\gamma)}(\theta) = \Delta_{LF} \cdot \frac{d\left(d\sigma_{nf,n'(\gamma)}^{\{0\}}(\theta)\middle/d\Omega\right)}{d\theta} \middle/ \left(d\sigma_{nf,n'(\gamma)}^{\{0\}}(\theta)\middle/d\Omega\right) = \Delta_{LF} \cdot \frac{dP_{n'(\gamma)}^{\{0\}}(\theta)}{d\theta} \middle/ P_{n'(\gamma)}^{\{0\}}(\theta). \quad (23)$$

Г.В. Вальский, А.М. Гагарский, И.С. Гусева и др. // Изв.РАН, Сер.физ. 2010, Т.74, 803.

Taking into account the even nature of the experimental angular distribution of prompt neutrons and gamma quanta $P_{n',\gamma}^{\{0\}}(\theta)$ and, consequently, the odd nature of the quantity $\dfrac{dP_{n',\gamma}^{\{0\}}(\theta)}{d\theta}$ with respect to the transformation $\theta \rightarrow \pi - \theta$, we can obtain the following formulas:

$$\left(\beta_{nf,n',\gamma}(\theta)\right)_3 = 0, \quad \left(\beta_{nf,n',\gamma}(\theta)\right)_5 = \Delta_{LF}\frac{dP_{n',\gamma}^{\{0\}}(\theta)}{d\theta}. \tag{24}$$
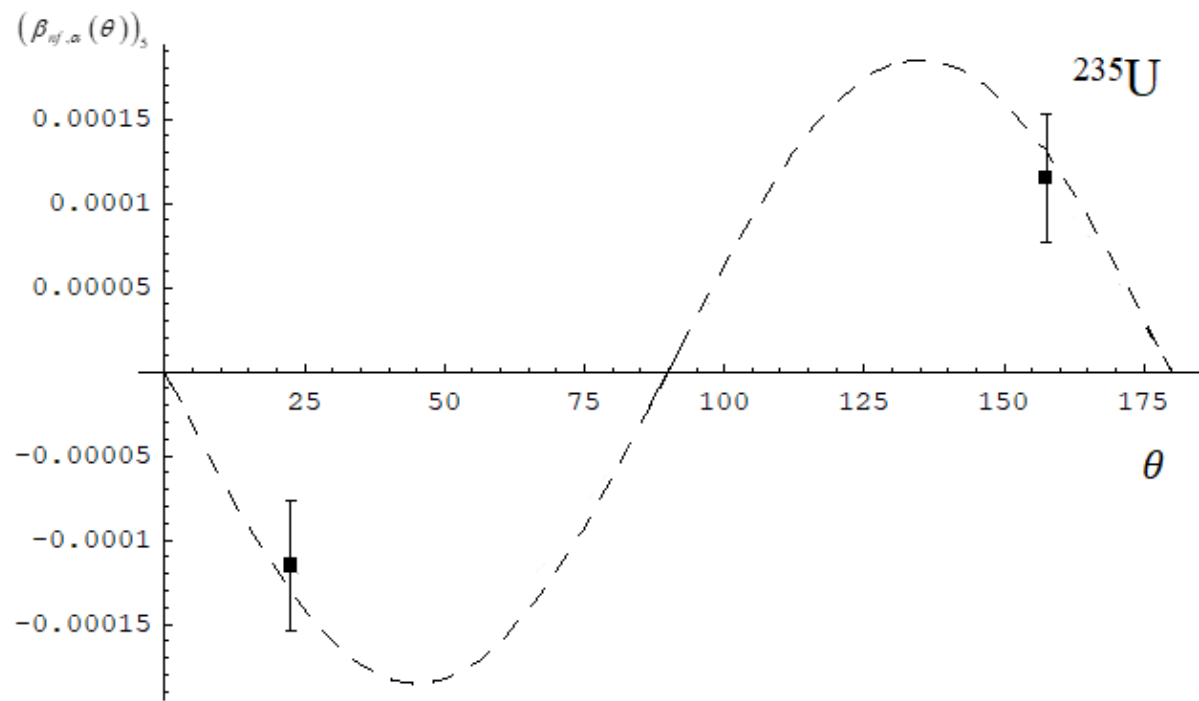
Fig. 23. Experimental (black squares) and calculated (short dotted line - semiclassical approach) values of $\left(\beta_{nf,n'}(\theta)\right)_5$ in the case of the ^{235}U target nucleus.
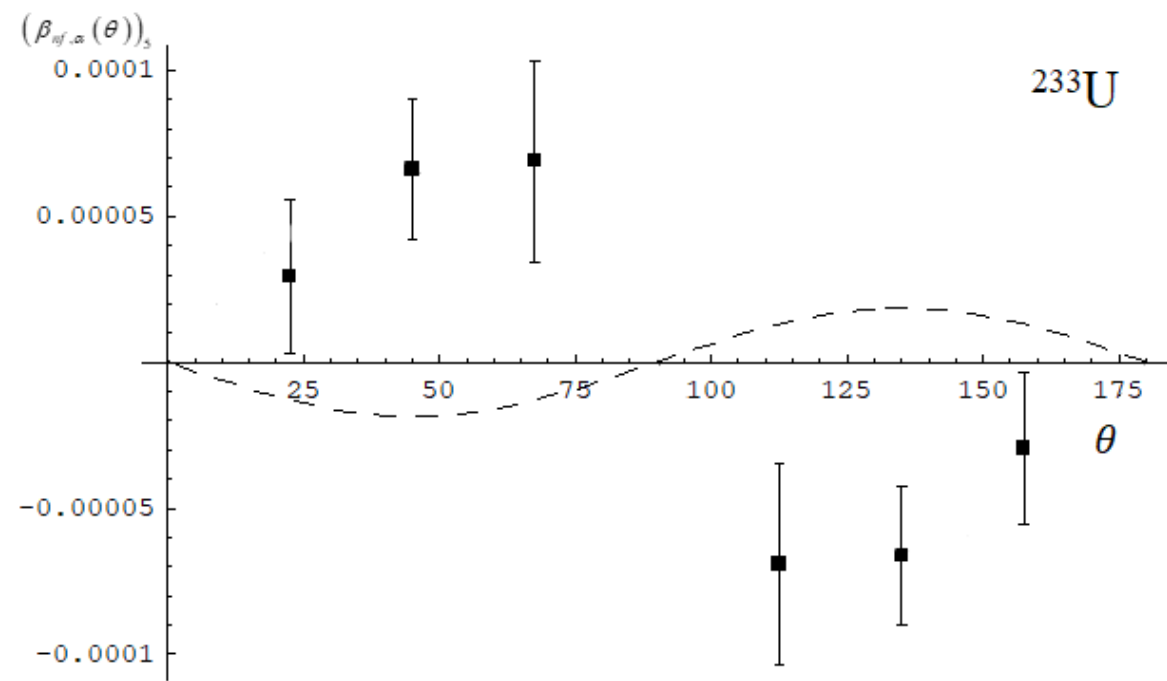
Fig. 24. Experimental (black squares) and calculated (short dotted line - semiclassical approach) values of $\left(\beta_{nf,\gamma}(\theta)\right)_5$ in the case of the ^{233}U target nucleus.
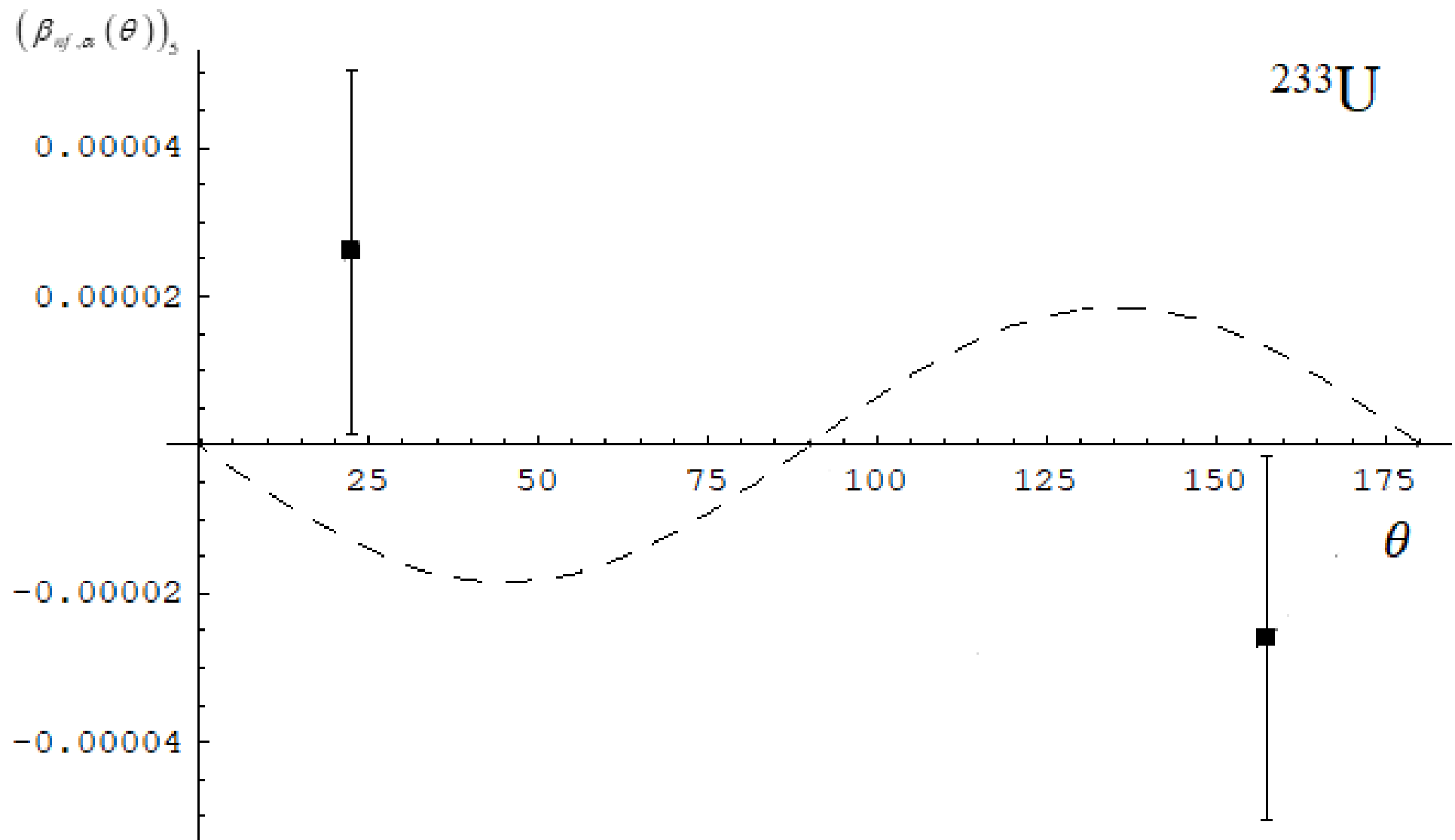
Fig. 25. Experimental (black squares) and calculated (short dotted line - semiclassical approach and long dotted line - quantum approach) values of $\left(\beta_{nf,n'}(\theta)\right)_5$ in the case of the target nucleus ^{233}U.

Section 3

Description of the characteristics of triple and quintuple correlators in the differential cross sections for fission reactions of unoriented target nuclei by cold polarized neutrons with the emission of prescission and evaporative light particles in the framework of the quantum theory of fission.

$$H^{\text{Cor}} = -\frac{\text{h}^2}{2\mathfrak{I}_0}\left(\hat{J}_+\hat{l}_- + \hat{J}_-\hat{l}_+\right) - \frac{\text{h}^2}{2\mathfrak{I}_0}\left(\hat{J}_+\hat{L}_- + \hat{J}_-\hat{L}_+\right), \qquad (25)$$

where $\mathfrak{I}_0$ is the moment of inertia of the axially symmetric CFN, which increases with the expansion of fission products.

$$\hat{J}_\pm = \hat{J}_1 \pm i\hat{J}_2; \quad \hat{l}_\pm = \hat{l}_1 \pm i\hat{l}_2; \quad \hat{L}_\pm = \hat{L}_1 \pm i\hat{L}_2.$$

$$\Psi^{sJ_sM_s}\left(x\right) = \Psi_0^{sJ_sM_s}\left(x\right) + \int G\left(x,x'\right)\, H^{\mathrm{Cor}}\left(x'\right)\Psi_0^{sJ_sM_s}\left(x'\right)dx', \qquad (26)$$

$$\left(d\sigma_{nf,p}^{\{1\}}\left(\theta\right)\big/d\Omega\right)_{3(5)} = \Delta_{p,3(5)}\frac{d}{d\theta}\left(d\sigma_{nf,p}^{\{0\}}\left(\theta\right)\big/d\Omega\right)_{ev(odd)}. \qquad (27)$$

Кадменский С.Г., Титова Л.В., Бунаков В.Е. // ЯФ. 2019. Т. 82. С. 239-248.

$$\Delta_{\alpha,3(5)} = \sum_{sJ_s s'J_{s'}K_s c} g_{cK_s}^{sJ_s s'J_{s'}} \tau\omega\left(K_s, J_s, J_{s'}\right) \sin\left(\delta_{sJ_s s'J_{s'}} + \delta_{3(5)}^{cor} - \delta^0\right) - \tag{28}$$

$$- \sum_{sJ_s s'J_{s'}K_s c} g_{cK_s}^{sJ_s s'J_{s'}} \tau\omega\left(K_s, J_s, J_{s'}\right) \sin\left(\delta_{sJ_s s'J_{s'}}\right);$$

$$\Delta_{n'(\gamma),5} = \sum_{sJ_s s'J_{s'}K_s c} g_{cK_s}^{sJ_s s'J_{s'}} \tau\omega\left(K_s, J_s, J_{s'}\right) \sin\left(\delta_{sJ_s s'J_{s'}}\right). \tag{29}$$

$$\left(\beta_{nf,p}^0\left(\theta\right)\right)_{3(5)} = \Delta_{p,3(5)} \frac{d}{d\theta}\left(P_{p,ev(odd)}^{\{0\}}\left(\theta\right)\right). \tag{30}$$

Кадменский С.Г., Титова Л.В., Бунаков В.Е. // ЯФ. 2019. Т. 82. С. 239-248.

Table 3

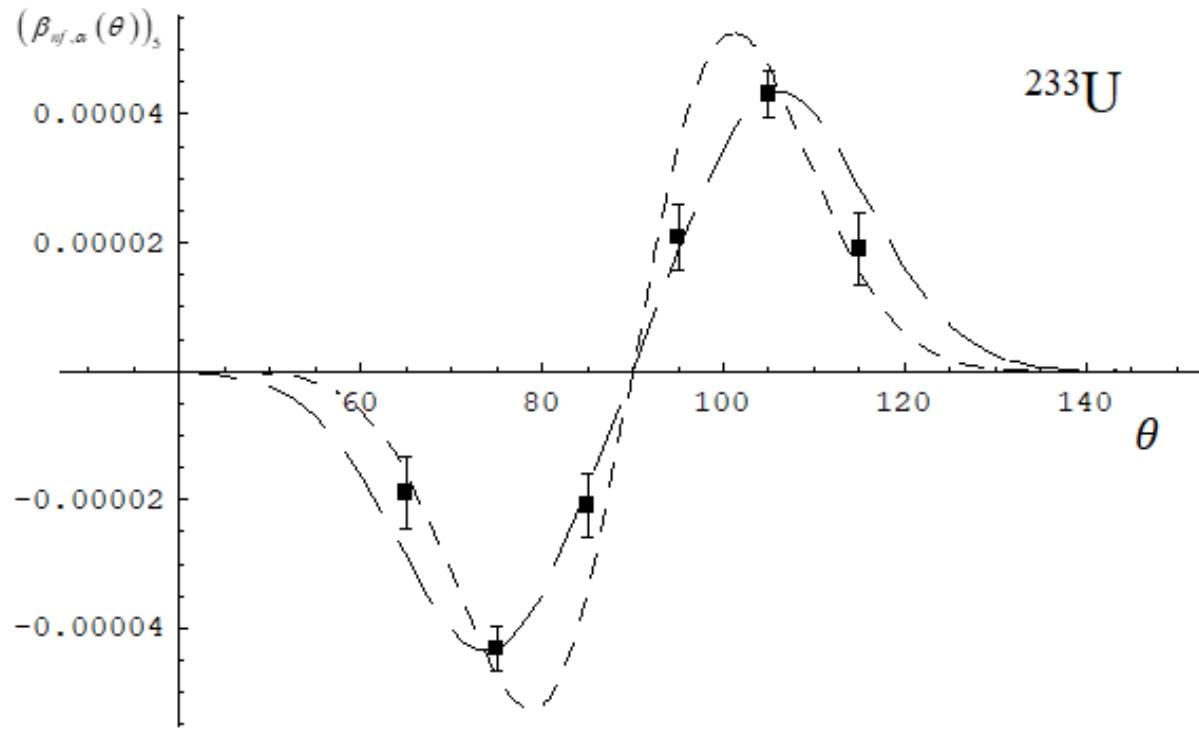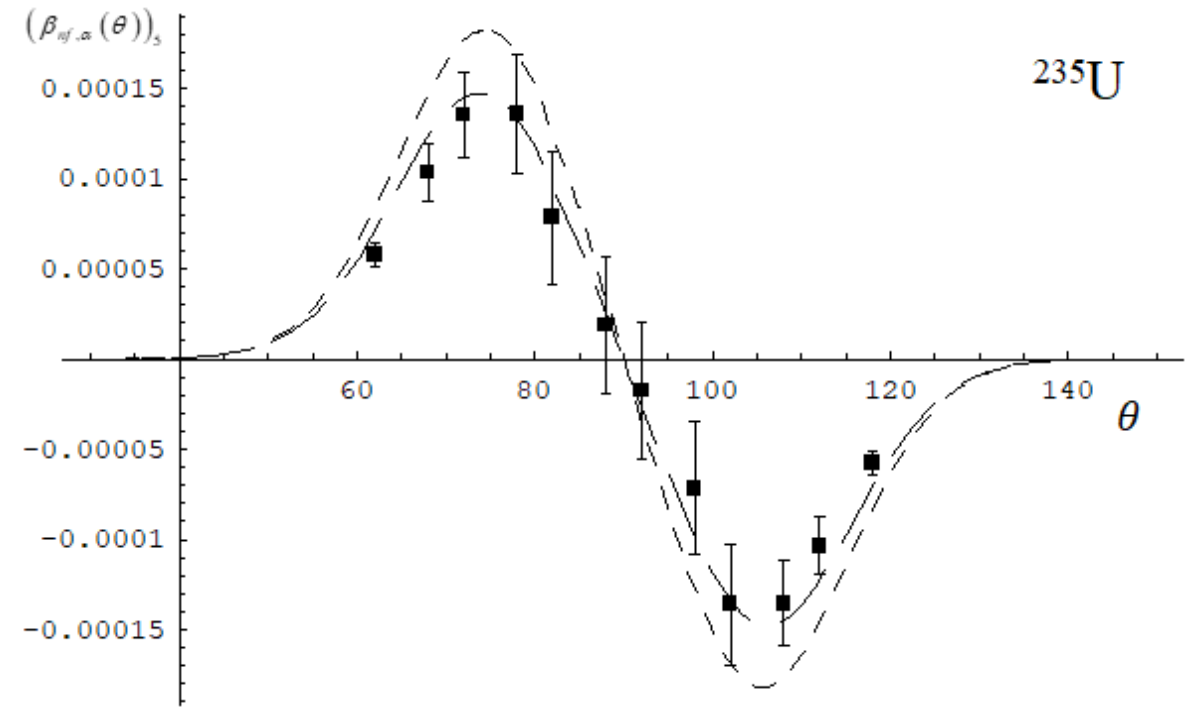| Target nucleus	$\Delta_{\alpha,3} \cdot 10^{-3}$	$\Delta_{\alpha,5} \cdot 10^{-3}$	$\Delta_{\alpha} \cdot 10^{-3}$	$\Delta_{\gamma,5} \cdot 10^{-3}$	$\Delta_{n',5} \cdot 10^{-3}$
^{233}U	0.5	-0.5	0.18	-0.48	-0.78
^{235}U	1.4	1.9	1.9	1.6	3.3
^{239}Pu	0.19	0.1	0.17		
^{241}Pu	0.25	0.6	0.41		

Fig. 26. Experimental (black squares) and calculated (short dotted line - semiclassical approach and long dotted line - quantum approach) values of $\left(\beta_{nf,\alpha}(\theta)\right)_s$ in the case of the target nucleus ^{233}U.
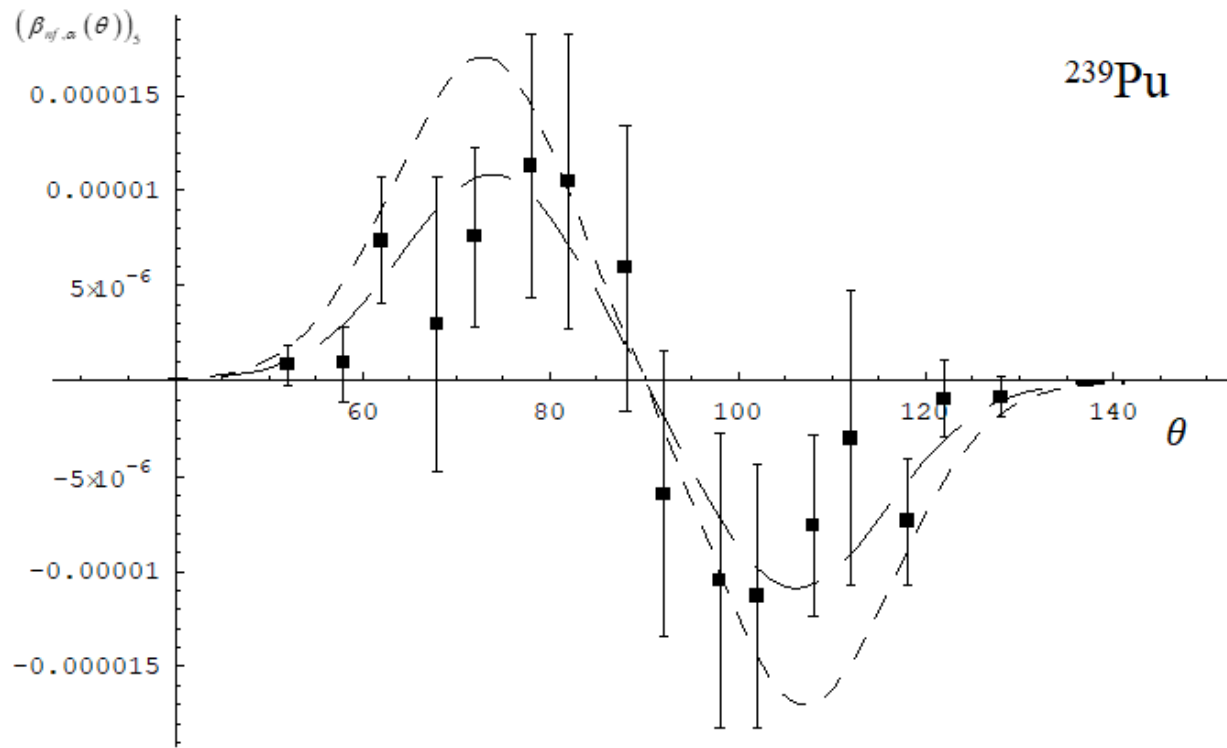

Fig. 27. Experimental (black squares) and calculated (short dotted line - semiclassical approach and long dotted line - quantum approach) values of $\left(\beta_{nf,\alpha}(\theta)\right)_s$ in the case of the ^{235}U target nucleus.

Fig. 28. Experimental (black squares) and calculated (short dotted line - semiclassical approach and long dotted line - quantum approach) values of $\left(\beta_{nf,\alpha}(\theta)\right)_s$ in the case of the ^{239}Pu target nucleus.
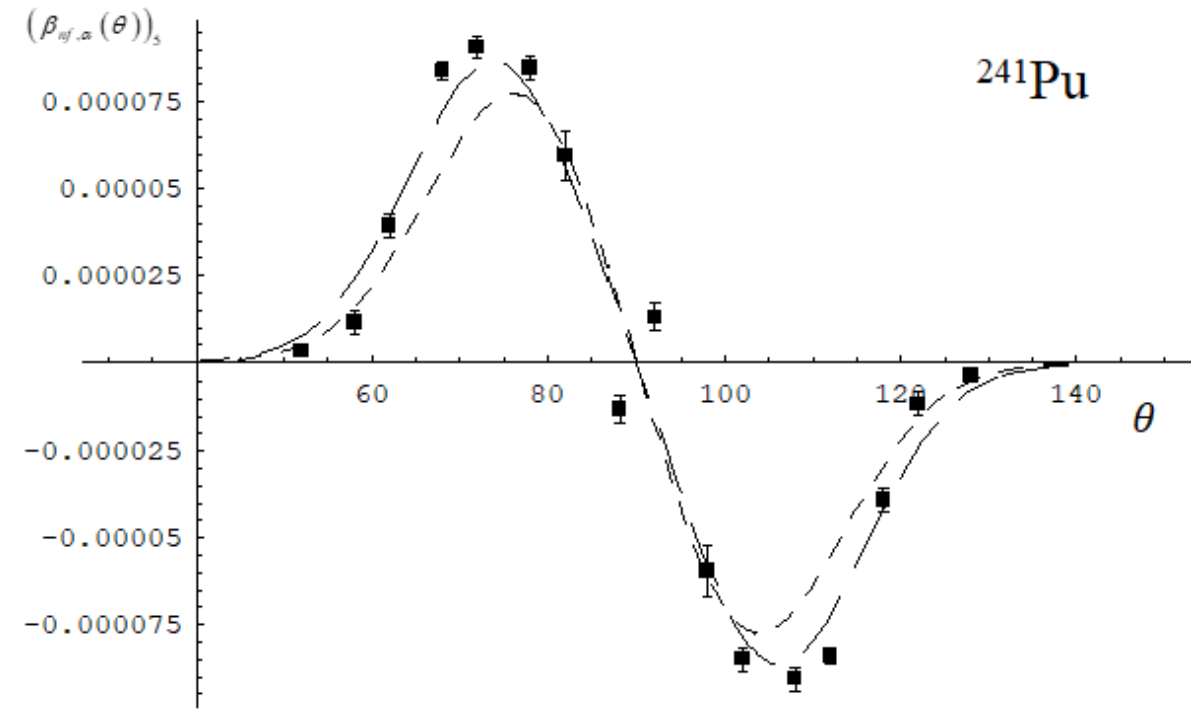
Fig. 29. Experimental (black squares) and calculated (short dotted line - semiclassical approach and long dotted line - quantum approach) values of $\left(\beta_{nf,\alpha}(\theta)\right)_s$ in the case of the target nucleus ^{241}Pu.
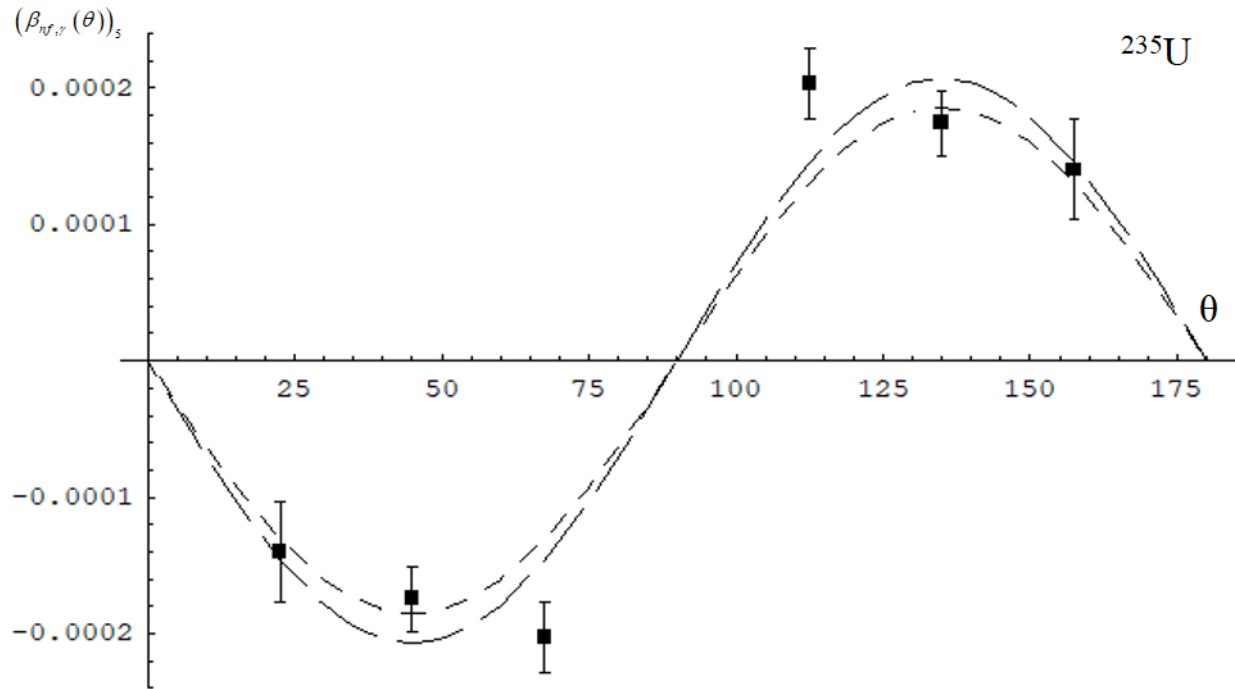
Fig. 30. Experimental (black squares) and calculated (short dotted line - semiclassical approach and long dotted line - quantum approach) values of $\left(\beta_{nf,\gamma}(\theta)\right)_5$ in the case of the target nucleus ^{235}U.
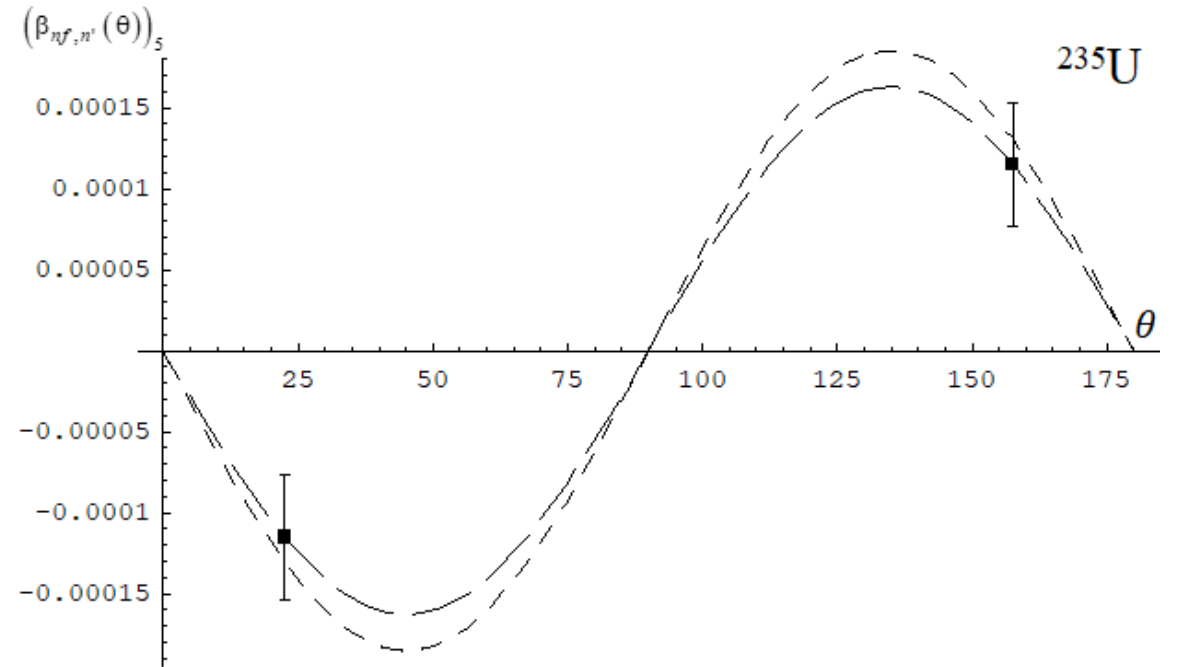

Fig. 31. Experimental (black squares) and calculated (short dotted line - semiclassical approach and long dotted line - quantum approach) values of $\left(\beta_{nf,n'}(\theta)\right)_5$ in the case of the target nucleus ^{235}U.

Fig. 32. Experimental (black squares) and calculated (short dotted line - semiclassical approach and long dotted line - quantum approach) values of $\left(\beta_{nf,\gamma}(\theta)\right)_5$ in the case of the target nucleus ^{233}U.
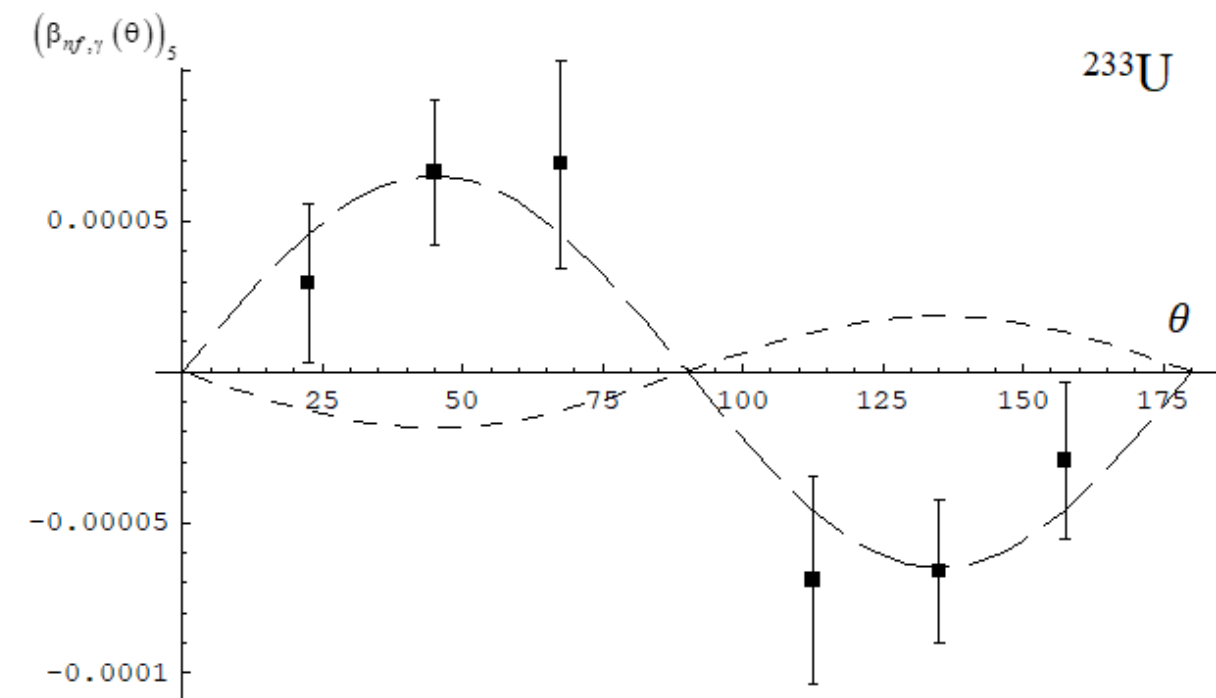
Fig. 33. Experimental (black squares) and calculated (short dotted line - semiclassical approach and long dotted line - quantum approach) values of $\left(\beta_{nf,n'}(\theta)\right)_5$ in the case of the target nucleus ^{233}U.
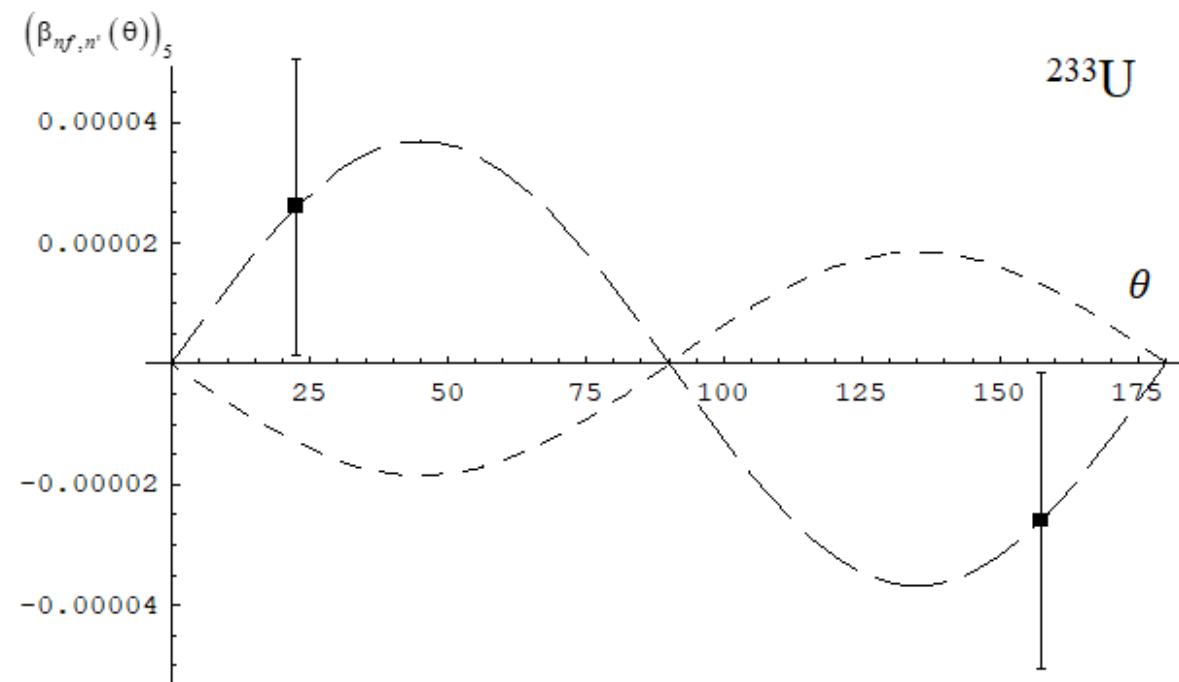
Fig. 34. Experimental (black squares) and calculated (short dotted line - semiclassical approach and long dotted line - quantum approach) values of $\left(\beta_{nf,\alpha}(\theta)\right)_3$ in the case of the target nucleus ^{233}U.

Fig. 35. Experimental (black squares) and calculated (short dotted line - semiclassical approach and long dotted line - quantum approach) values of $\left(\beta_{nf,\alpha}(\theta)\right)_3$ in the case of the target nucleus ^{235}U.
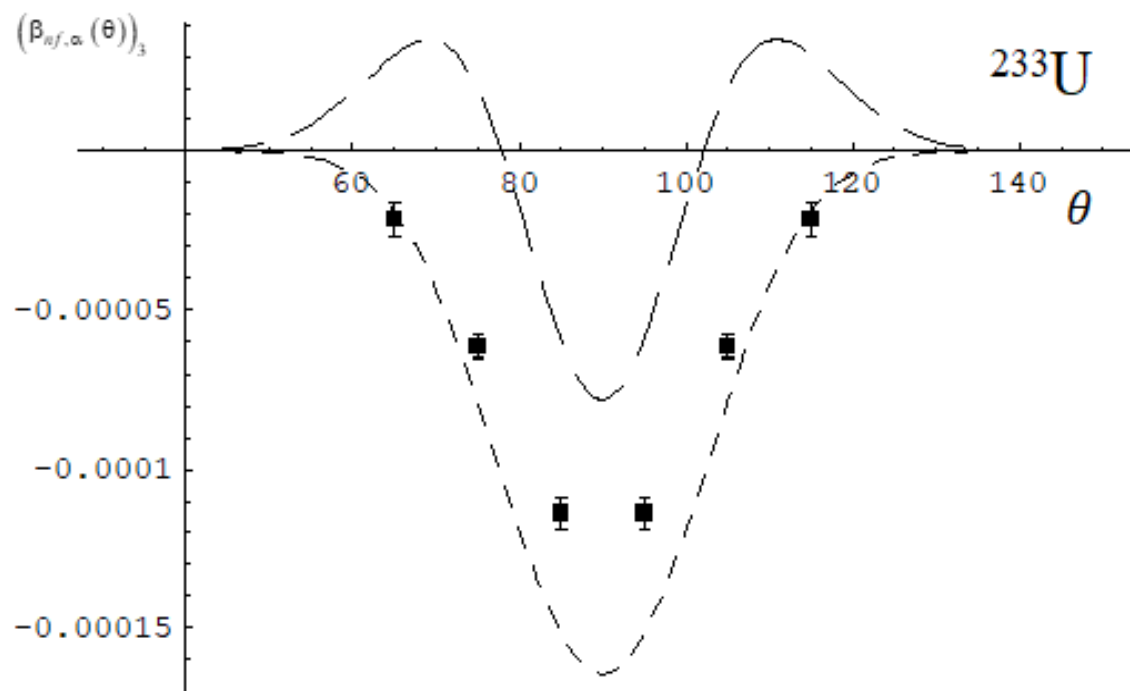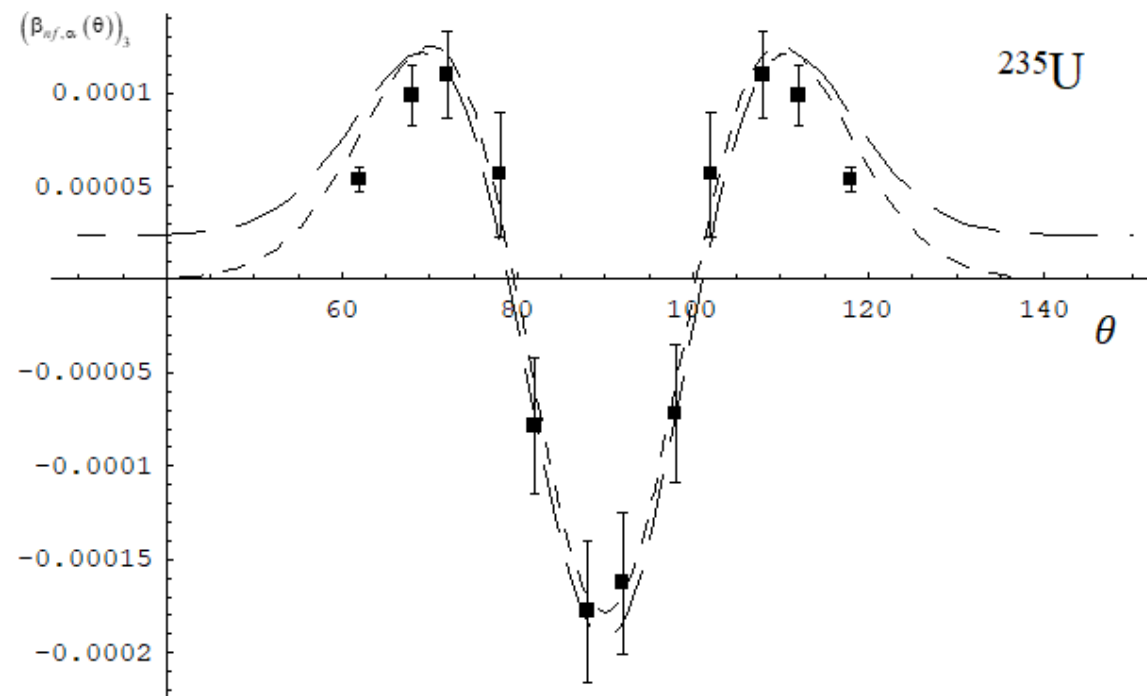
Fig. 36. Experimental (black squares) and calculated (short dotted line - semiclassical approach and long dotted line - quantum approach) values of $\left(\beta_{nf,\alpha}(\theta)\right)_3$ in the case of the ^{239}Pu target nucleus.
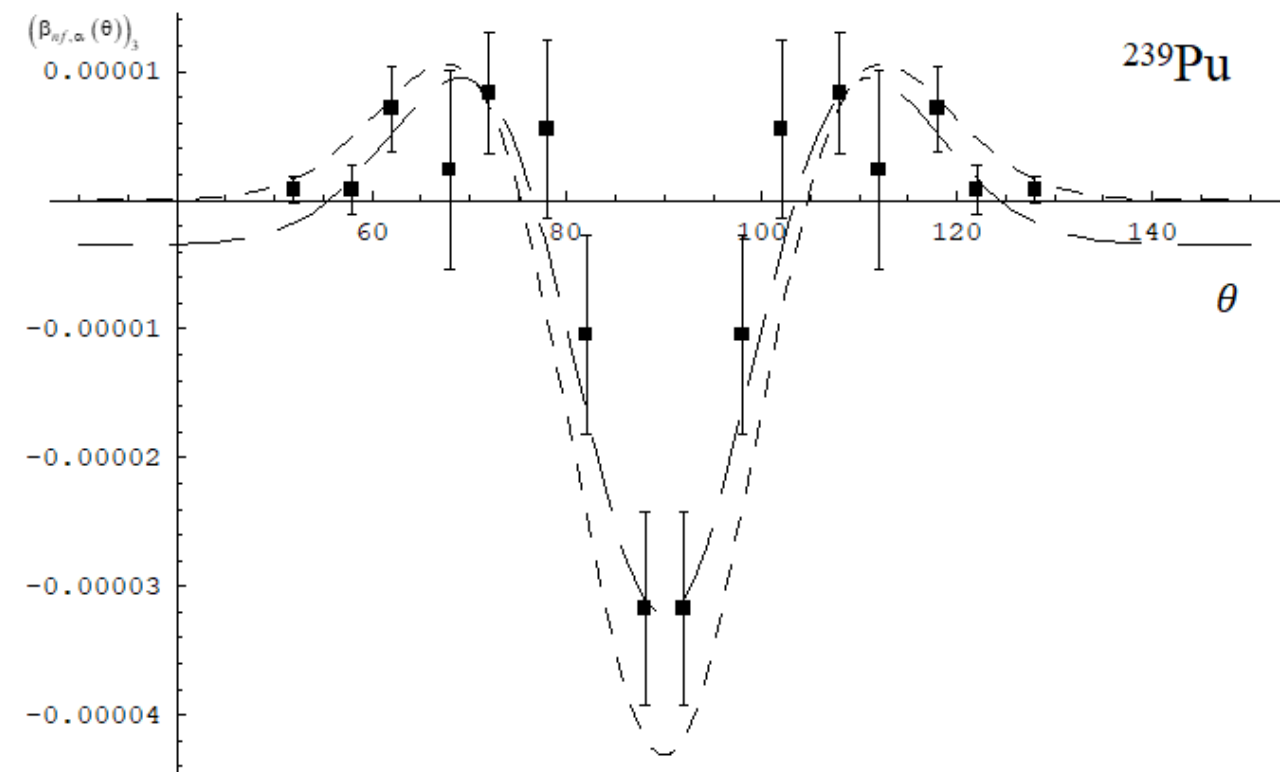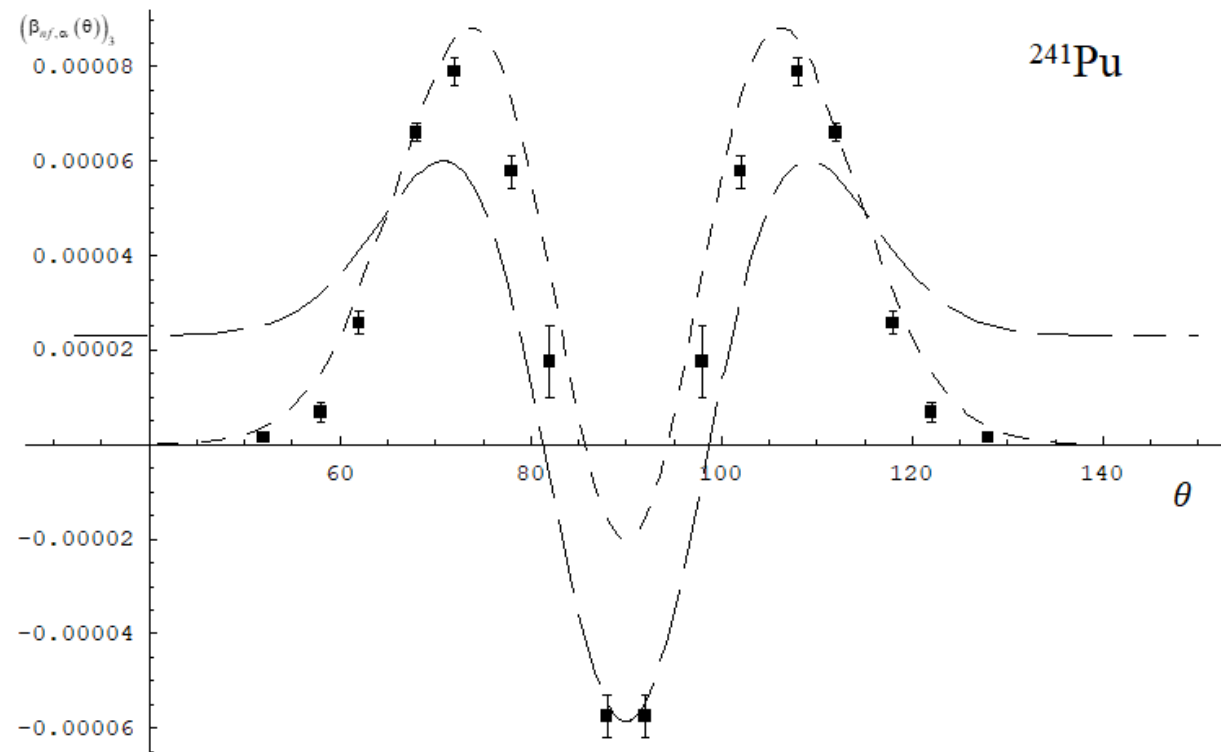

Fig. 37. Experimental (black squares) and calculated (short dashed line - semiclassical approach and long dashed line - quantum approach) values of $\left(\beta_{nf,\alpha}(\theta)\right)_3$ in the case of the ^{241}Pu target nucleus.

$$\left(\beta_{nf,\alpha}(\theta)\right)_3 = \Delta_{\alpha,3}\frac{d}{d\theta}\left(P_{\alpha,odd}^{\{0\}}(\theta)\right)+\left(\beta_{nf,\alpha}\right)_3 = \left(\beta_{nf,\alpha}^0(\theta)\right)_3 +\left(\beta_{nf,\alpha}\right)_3. \qquad (31)$$

Table 8

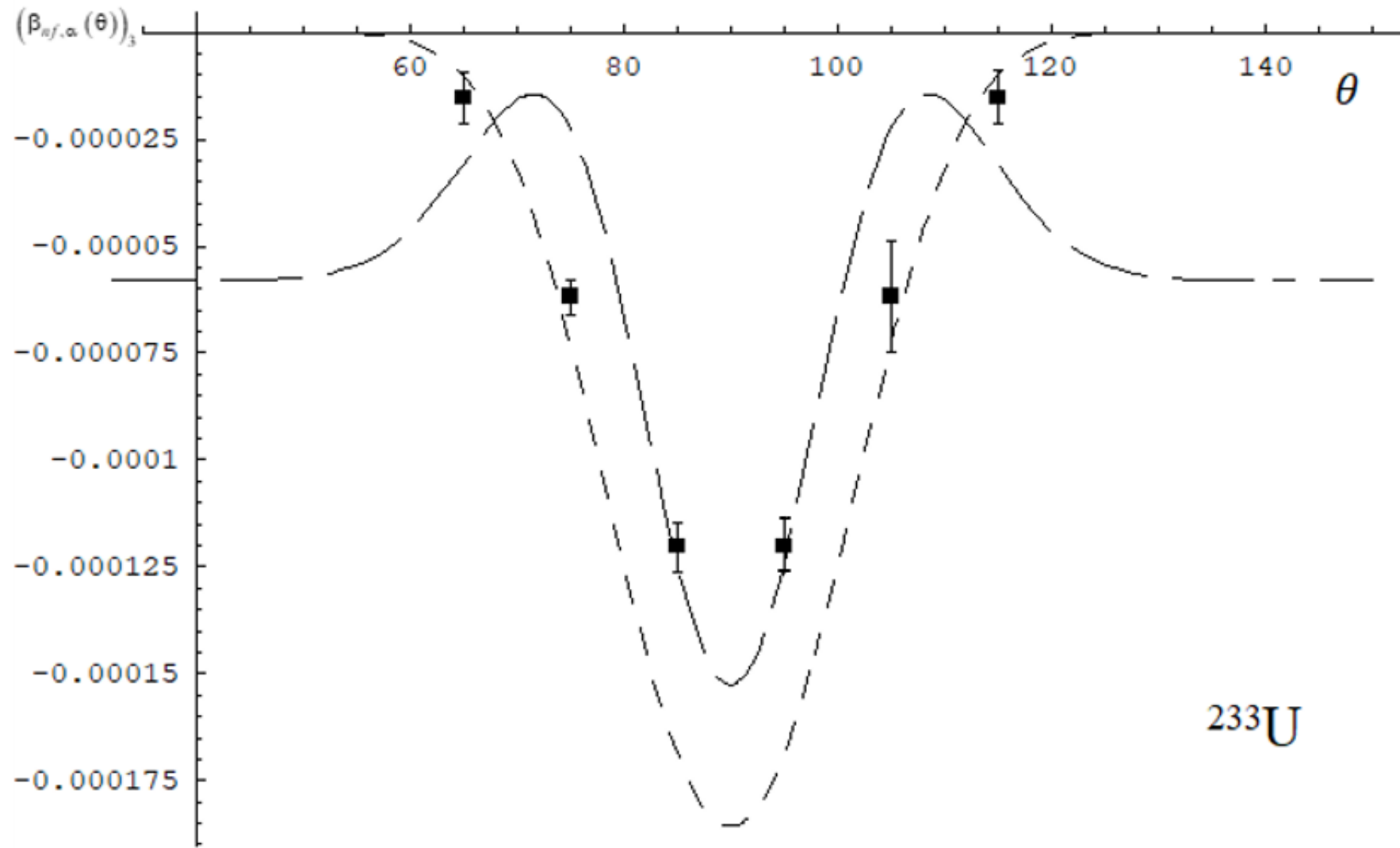| Target nucleus	$\overset{o}{\Delta}_{\alpha,3}\cdot 10^{-3}$	$\Delta_{\alpha,3}\cdot 10^{-3}$	$\Delta_{\alpha}\times 10^{-3}$	$\left(\tilde{\beta}_{nf,\alpha}\right)_3\cdot 10^{-3}$
^{233}U	0.6	0.5	0.18	-0.045
^{235}U	1.5	1.4	1.9	0.02
^{239}Pu	0.19	0.19	0.17	-0.002
^{241}Pu	0.33	0.25	0.41	0.023

Fig. 38. Experimental (black squares) and calculated (short dotted line - semiclassical approach and long dotted line - quantum approach) values of $\left(\beta_{nf,\alpha}(\theta)\right)_3$ in the case of the ^{233}U nucleus.

Conclusions

The existence of a single mechanism for the appearance of triple $\left(\overrightarrow{\sigma_n}, \lfloor \vec{k}_{\text{LF}}, \vec{k}_\alpha \rfloor\right)$ and quintuple $\left(\overrightarrow{\sigma_n}, \lfloor \vec{k}_{\text{LF}}, \vec{k}_\alpha \rfloor\right)(\vec{k}_{\text{LF}}, \vec{k}_\alpha)$ P-even T-odd scalar correlations in the differential cross sections for reactions of triple fission of nuclei by cold polarized neutrons with the emission of alpha particles, due to the Coriolis interaction of the total spin of the rotating compound fissile nucleus, not only with the orbital moments of fission fragments, has been confirmed, but also with even and odd orbital moments of alpha particles, which form the corresponding components of the amplitudes of their unperturbed angular distributions.

An additional mechanism is proposed associated with the violation of the axial - symmetry of the CFS, due to the influence of transverse bending - vibrations of the CFS in the vicinity of its discontinuity point, and the appearance of the Coriolis interaction due to this, associated with the rotation of the CFS with an angular velocity ω, directed along the axis of symmetry CFS excluding transverse bending – oscillations.

It is shown that for the calculated rotation angles there is agreement between the absolute values and signs of angles $\Delta_{\alpha,5}$ and $\Delta_{n',\gamma,5}$ in the case of both uranium isotopes ^{233}U and ^{235}U. The appearance of negative signs of rotation angles $\Delta_{\alpha,5}$ and $\Delta_{n',\gamma,5}$ for quintuple correlators in the case of the ^{233}U target nucleus is demonstrated, in contrast to the positive signs of these angles for all other target nuclei, which may be due to the influence of the interference of fission amplitudes of neutron resonance states of the composite fissile nucleus sJ_s and $s'J_{s'}$ with different values of sJ_s and $s'J_{s'}$.

The connection of P-even T-odd asymmetries in the angular distributions of prompt neutrons and γ - quanta with respect to the direction of emission of nuclear fission fragments by cold polarized neutrons with quintuple $\left(\overrightarrow{\sigma_n},\left[\vec{k}_{\mathrm{LF}},\vec{k}_{n',\gamma}\right]\right)\left(\vec{k}_{\mathrm{LF}},\vec{k}_{n',\gamma}\right)$ scalar correlations due to the influence of the Coriolis interaction of the total spin of a rotating fissile system with the orbital moments of fission fragments is demonstrated.

Thank you for your attention!